

Golden Littlest Seesaw

Gui-Jun Ding^{1*}, Stephen F. King^{2†}, Cai-Chang Li^{1‡}

¹*Interdisciplinary Center for Theoretical Study and Department of Modern Physics,
University of Science and Technology of China, Hefei, Anhui 230026, China*

²*Physics and Astronomy, University of Southampton, Southampton, SO17 1BJ, U.K.*

Abstract

We propose and analyse a new class of Littlest Seesaw models, with two right-handed neutrinos in their diagonal mass basis, based on preserving the first column of the Golden Ratio mixing matrix. We perform an exhaustive analysis of all possible remnant symmetries of the group A_5 which can be used to enforce various vacuum alignments for the flavon controlling solar mixing, for two simple cases of the atmospheric flavon vacuum alignment. The solar and atmospheric flavon vacuum alignments are enforced by *different* remnant symmetries. We examine the phenomenological viability of each of the possible Littlest Seesaw alignments in A_5 , which preserve the first column of the Golden ratio mixing matrix, using figures and extensive tables of benchmark points and comparing our predictions to a recent global analysis of neutrino data. We also repeat the analysis for an alternative form of Golden Ratio mixing matrix.

*E-mail: dinggj@ustc.edu.cn

†E-mail: king@soton.ac.uk

‡E-mail: lcc0915@mail.ustc.edu.cn

1 Introduction

Massive neutrinos together with neutrino oscillations has been firmly established, and it is unique experimental evidence for physics beyond the standard model. All the three lepton mixing angles θ_{12} , θ_{13} and θ_{23} and the mass squared differences $\delta m^2 \equiv m_2^2 - m_1^2$ and $\Delta m^2 \equiv m_3^2 - (m_1^2 + m_2^2)/2$ has been precisely measured in a large number of neutrino oscillation experiments. At present the 3σ ranges of these mixing parameters are determined to be [1]

$$0.250 \leq \sin^2 \theta_{12} \leq 0.354, \quad 0.0190 \leq \sin^2 \theta_{13} \leq 0.0240, \quad 0.381 \leq \sin^2 \theta_{23} \leq 0.615, \quad (1.1)$$
$$6.93 \times 10^{-5} \text{eV}^2 \leq \delta m^2 \leq 7.96 \times 10^{-5} \text{eV}^2, \quad 2.411 \times 10^{-3} \text{eV}^2 \leq \Delta m^2 \leq 2.646 \times 10^{-3} \text{eV}^2,$$

for normal ordering (NO) neutrino mass spectrum, and similar results are obtained for inverted ordering (IO) spectrum. Non-Abelian discrete finite groups have been widely used to explain the lepton mixing angles as well as CP violating phases, see Refs. [2–7] for reviews.

The most appealing possibility for the origin of neutrino mass seems to be the seesaw mechanism which, in its original formulation, involves heavy right-handed Majorana neutrinos [8]. The most minimal version of the seesaw mechanism involves one [9] or two right-handed neutrinos [10]. In order to reduce the number of free parameters still further to the smallest number possible, and hence increase predictivity, various approaches to the two right-handed neutrino seesaw model have been suggested, such as postulating one [11] or two [12] texture zeroes, however such two texture zero models are now phenomenologically excluded [13] for the case of a normal neutrino mass hierarchy considered here.

The minimal successful seesaw scheme with normal hierarchy is called the Littlest Seesaw (LS) model [14–16], although in fact, it represents a class of models. The LS models may be defined as two right-handed neutrino models with particularly simple patterns of Dirac mass matrix elements in the basis where both the charged lepton mass matrix and the two-right-handed neutrino mass matrix are diagonal. The Dirac mass matrix typically involves only one texture zero, but the number of parameters is reduced dramatically since each column of this matrix is controlled by a single parameter. In practice this is achieved by introducing a Non-Abelian discrete family symmetry, which is spontaneously broken by flavon fields with particular vacuum alignments governed by remnant subgroups of the family symmetry. Unlike the direct symmetry approach, where a common residual flavour and remnant CP symmetry is assumed in the neutrino sector, the Littlest Seesaw approach assumes a *different* residual flavour symmetry is preserved by each flavon, in the diagonal mass basis of two right-handed neutrinos, leading to a highly predictive set of possible alignments.

For example, in the original LS model [14–16], the lepton mixing matrix is predicted to be of the TM1 form in which the first column of the tri-bimaximal mixing matrix is preserved, but with the reactor angle and CP phases fixed by the same two parameters which fix the neutrino masses. This leads to a highly constrained model which is remarkably consistent with current data, but which can be tested in forthcoming neutrino experiments [17]. The LS approach may also be incorporated into grand unified models [18]. The success of the LS approach, raises the question of whether it is confined to TM1 mixing, or is of more general applicability. The present paper aims to address this question by considering a different mixing scheme within the same approach, namely the golden ratio (GR) mixing pattern [19, 20].

In this paper, we shall propose another viable class of LS models, namely the Golden Littlest seesaw (GLS). Although the golden ratio mixing [19, 20] is excluded by the measure-

ment of largish reactor mixing angle, the first column of U_{GR} may still be compatible with the experimental data. Inspired by the success of the LS approach for TM1 mixing, we would like to also preserve the first column vector of the GR mixing pattern in our GLS model. We shall perform an exhaustive analysis of all possible remnant symmetries of the group A_5 which can be used to enforce various vacuum alignments for the flavon controlling solar mixing, for two simple cases of the atmospheric flavon vacuum alignment, analogous to the procedure suggested in the LS approach based on S_4 . For each possibility we examine the phenomenological viability of the alignment, using figures and extensive benchmark points, comparing our predictions to a recent global analysis of neutrino data. We also repeat the analysis for an alternative form of Golden Ratio mixing matrix.

The layout of this paper is as follows. In section 2 we review GR mixing and the direct model building approach based on the group A_5 . In section 3 we then turn to the GLS approach, based on two right-handed neutrinos with the Dirac mass matrix controlled by flavon vacuum alignments which respect various remnant symmetries of A_5 , and examine the phenomenological viability of each case for a discrete choice of phase parameters. In section 4 we repeat the procedure for an alternative choice of GR matrix. Section 5 concludes the paper. We report the group theory of A_5 in Appendix A, and the technique details of diagonalizing a two dimensional symmetric matrix are shown in Appendix B.

2 Golden Ratio Mixing

2.1 Mixing matrix and Klein symmetry

Before the measurement of the reactor mixing angle, the golden ratio (GR) mixing pattern [19, 20] was a good leading order approximation and it predicted a zero reactor angle $\theta_{13} = 0$, maximal atmospheric mixing angle $\theta_{23} = 45^\circ$ and a solar mixing angle given by $\cot \theta_{12} = \phi$, where $\phi = (1 + \sqrt{5})/2$ is the golden ratio. Note that the golden ratio mixing differs from the tri-bimaximal mixing in the prediction for the solar mixing angle. The explicit form of the golden mixing matrix is given by

$$U_{GR} = \begin{pmatrix} -\sqrt{\frac{\phi}{\sqrt{5}}} & \sqrt{\frac{1}{\sqrt{5}\phi}} & 0 \\ \sqrt{\frac{1}{2\sqrt{5}\phi}} & \sqrt{\frac{\phi}{2\sqrt{5}}} & -\frac{1}{\sqrt{2}} \\ \sqrt{\frac{1}{2\sqrt{5}\phi}} & \sqrt{\frac{\phi}{2\sqrt{5}}} & \frac{1}{\sqrt{2}} \end{pmatrix}. \quad (2.1)$$

In the flavor basis where the charged lepton mass matrix m_l is diagonal with $m_l = \text{diag}(m_e, m_\mu, m_\tau)$, then the most general form of the neutrino matrix m_ν for the golden ratio mixing is

$$m_\nu = U_{GR} \text{diag}(m_1, m_2, m_3) U_{GR}^T = m_1 \Phi_1 \Phi_1^T + m_2 \Phi_2 \Phi_2^T + m_3 \Phi_3 \Phi_3^T, \quad (2.2)$$

where the light neutrino masses $m_{1,2,3}$ absorbing the Majorana phases are generally complex, and the vectors $\Phi_{1,2,3}$ are defined as

$$\Phi_1 = \sqrt{\frac{1}{2\sqrt{5}\phi}} \begin{pmatrix} -\sqrt{2}\phi \\ 1 \\ 1 \end{pmatrix}, \quad \Phi_2 = \sqrt{\frac{1}{2\sqrt{5}\phi}} \begin{pmatrix} \sqrt{2} \\ \phi \\ \phi \end{pmatrix}, \quad \Phi_3 = \frac{1}{\sqrt{2}} \begin{pmatrix} 0 \\ -1 \\ 1 \end{pmatrix}. \quad (2.3)$$

A unitary transformation $\nu_L \rightarrow G_\nu \nu_L$ of the left-handed Majorana neutrino fields leads to the transformation of the neutrino mass matrix $m_\nu \rightarrow G_\nu^T m_\nu G_\nu$. We can check that the above golden ratio neutrino mass matrix is invariant under the following transformations

$$G_{\nu_i}^T m_\nu G_{\nu_i} = m_\nu, \quad i = 1, 2, 3, \quad (2.4)$$

with

$$G_{\nu_1} = 2\Phi_1\Phi_1^\dagger - 1, \quad G_{\nu_2} = 2\Phi_2\Phi_2^\dagger - 1, \quad G_{\nu_3} = 2\Phi_3\Phi_3^\dagger - 1 \quad (2.5)$$

The three flavor symmetry transformations G_{ν_1} , G_{ν_2} and G_{ν_3} form a Klein group $K_4 \cong Z_2 \times Z_2$ and they fulfill

$$G_{\nu_i}^2 = \mathbf{1}, \quad G_{\nu_i} G_{\nu_j} = G_{\nu_j} G_{\nu_i} = G_{\nu_k} \quad \text{with } i \neq j \neq k. \quad (2.6)$$

Furthermore, the symmetry transformation G_l of the charged lepton mass matrix is determined by the condition $G_l^\dagger m_l^\dagger m_l G_l = m_l^\dagger m_l$, therefore G_l has to be a diagonal phase matrix. If we choose $G_l = \text{diag}(1, \rho, \rho^4)$ with $\rho = e^{2\pi i/5}$, the matrices G_l , G_{ν_1} , G_{ν_2} and G_{ν_3} would give rise to the group A_5 in the triplet representation [21]. According to the direct model building approach [4], if the flavor symmetry A_5 is broken to a Z_5 subgroup in the charged lepton sector and to Klein subgroup in the neutrino sector, the golden ratio mixing pattern would be obtained naturally [21].

2.2 Direct approach in A_5

In both the direct approach and indirect approach, the basis principle of the flavor symmetry model building is the same, that is the different sectors of the Lagrangian preserve different residual subgroups of the flavor symmetry while the whole Lagrangian completely breaks the flavor symmetry. In order to more clearly understand the idea of the GLS, we shall briefly recapitulate the direct approach to the GR mixing from A_5 flavor symmetry before presenting our GLS within the indirect approach in the following section.

We first recall that A_5 is the even permutation group of five objects. Geometrically A_5 is the symmetry group of the icosahedron. The A_5 group can be generated by two generators S and T which satisfy the following multiplication rules

$$S^2 = T^5 = (ST)^3 = 1. \quad (2.7)$$

The A_5 group has five irreducible representations: one single $\mathbf{1}$, two triplets $\mathbf{3}$ and $\mathbf{3}'$, one four-dimensional representation $\mathbf{4}$ and one five-dimensional representation $\mathbf{5}$. The explicit form of the representation matrices for the generators S and T are collected in table 1. The interested readers can refer to Ref. [22] for detailed group theory of A_5 and Clebsch-Gordan coefficients. The interplay between A_5 flavor symmetry and lepton mixing has been extensively studied in the literature [21–28]. We find that the representation matrices of the generators S and T in $\mathbf{3}'$ exactly coincide with those of $T^3 S T^2 S T^3$ and T^2 respectively in $\mathbf{3}$. This implies that the set of all matrices describing the representations $\mathbf{3}$ and $\mathbf{3}'$ are the same. Therefore the same results would be obtained no matter if the left-handed leptons transform as $\mathbf{3}$ or $\mathbf{3}'$ of A_5 . Without loss of generality, We shall assign the three generations of left-handed leptons to the triplet $\mathbf{3}$ in the following.

	S	T
1	1	1
3	$\frac{1}{\sqrt{5}} \begin{pmatrix} 1 & -\sqrt{2} & -\sqrt{2} \\ -\sqrt{2} & -\phi & 1/\phi \\ -\sqrt{2} & 1/\phi & -\phi \end{pmatrix}$	$\begin{pmatrix} 1 & 0 & 0 \\ 0 & \rho & 0 \\ 0 & 0 & \rho^4 \end{pmatrix}$
3'	$\frac{1}{\sqrt{5}} \begin{pmatrix} -1 & \sqrt{2} & \sqrt{2} \\ \sqrt{2} & -1/\phi & \phi \\ \sqrt{2} & \phi & -1/\phi \end{pmatrix}$	$\begin{pmatrix} 1 & 0 & 0 \\ 0 & \rho^2 & 0 \\ 0 & 0 & \rho^3 \end{pmatrix}$
4	$\frac{1}{\sqrt{5}} \begin{pmatrix} 1 & 1/\phi & \phi & -1 \\ 1/\phi & -1 & 1 & \phi \\ \phi & 1 & -1 & 1/\phi \\ -1 & \phi & 1/\phi & 1 \end{pmatrix}$	$\begin{pmatrix} \rho & 0 & 0 & 0 \\ 0 & \rho^2 & 0 & 0 \\ 0 & 0 & \rho^3 & 0 \\ 0 & 0 & 0 & \rho^4 \end{pmatrix}$
5	$\frac{1}{5} \begin{pmatrix} -1 & \sqrt{6} & \sqrt{6} & \sqrt{6} & \sqrt{6} \\ \sqrt{6} & 1/\phi^2 & -2\phi & 2/\phi & \phi^2 \\ \sqrt{6} & -2\phi & \phi^2 & 1/\phi^2 & 2/\phi \\ \sqrt{6} & 2/\phi & 1/\phi^2 & \phi^2 & -2\phi \\ \sqrt{6} & \phi^2 & 2/\phi & -2\phi & 1/\phi^2 \end{pmatrix}$	$\begin{pmatrix} 1 & 0 & 0 & 0 & 0 \\ 0 & \rho & 0 & 0 & 0 \\ 0 & 0 & \rho^2 & 0 & 0 \\ 0 & 0 & 0 & \rho^3 & 0 \\ 0 & 0 & 0 & 0 & \rho^4 \end{pmatrix}$

Table 1: The representation matrices of the generators S and T for the five irreducible representations of A_5 group in the basis which is convenient for discussing the Golden ratio mixing pattern, where $\rho = e^{2\pi i/5}$ is the fifth root of unit.

In the direct approach, the A_5 flavor symmetry group is assumed to be broken to a abelian subgroup G_l such as $G_l = Z_5^T$. As a consequence the charged lepton mass matrix m_l is invariant under the action of the element T , i.e.

$$\rho_{\mathbf{3}}^\dagger(T) m_l^\dagger m_l \rho_{\mathbf{3}}(T) = m_l^\dagger m_l. \quad (2.8)$$

This implies that the unitary transformation U_l which diagonalizes the charged lepton mass matrix $U_l^\dagger(T) m_l^\dagger m_l U_l = \text{diag}(m_e^2, m_\mu^2, m_\tau^2)$ has the property

$$U_l^\dagger \rho_{\mathbf{3}}(T) U_l = \text{diag}(1, e^{i\frac{2\pi}{5}}, -e^{i\frac{3\pi}{5}}). \quad (2.9)$$

Since the generator T is diagonal with $\rho_{\mathbf{3}}(T) = \text{diag}(1, e^{i\frac{2\pi}{5}}, -e^{i\frac{3\pi}{5}})$ in our working basis, U_l has to be a unit matrix,

$$U_l = \begin{pmatrix} 1 & 0 & 0 \\ 0 & 1 & 0 \\ 0 & 0 & 1 \end{pmatrix}. \quad (2.10)$$

As a consequence, the lepton mixing completely arises from the neutrino mixing. The A_5 flavor symmetry is broken down to a Klein subgroup G_ν in the neutrino sector in the paradigm of direct approach. Here we choose $G_\nu = K_4^{(S, T^3 ST^2 ST^3)}$ whose representation

matrices in the chosen basis are

$$\begin{aligned}
\rho_{\mathbf{3}}(S) &= \frac{1}{\sqrt{5}} \begin{pmatrix} 1 & -\sqrt{2} & -\sqrt{2} \\ -\sqrt{2} & -\phi & 1/\phi \\ -\sqrt{2} & 1/\phi & -\phi \end{pmatrix}, \\
\rho_{\mathbf{3}}(T^3 ST^2 ST^3) &= \frac{1}{\sqrt{5}} \begin{pmatrix} -1 & \sqrt{2} & \sqrt{2} \\ \sqrt{2} & -1/\phi & \phi \\ \sqrt{2} & \phi & -1/\phi \end{pmatrix} \\
\rho_{\mathbf{3}}(T^3 ST^2 ST^3 S) &= - \begin{pmatrix} 1 & 0 & 0 \\ 0 & 0 & 1 \\ 0 & 1 & 0 \end{pmatrix}, \tag{2.11}
\end{aligned}$$

Then the neutrino diagonalization matrix U_ν turns out to be the golden ratio mixing pattern [21–24],

$$U_{GR} = \begin{pmatrix} -\sqrt{\frac{\phi}{\sqrt{5}}} & \sqrt{\frac{1}{\sqrt{5}\phi}} & 0 \\ \sqrt{\frac{1}{2\sqrt{5}\phi}} & \sqrt{\frac{\phi}{2\sqrt{5}}} & -\frac{1}{\sqrt{2}} \\ \sqrt{\frac{1}{2\sqrt{5}\phi}} & \sqrt{\frac{\phi}{2\sqrt{5}}} & \frac{1}{\sqrt{2}} \end{pmatrix}. \tag{2.12}$$

Notice that the three column vectors $\Phi_{1,2,3}$ of the GR mixing preserve three different Z_2 subgroups of A_5 ,

$$\rho_{\mathbf{3}}(S)\Phi_1 = \Phi_1, \quad \rho_{\mathbf{3}}(T^3 ST^2 ST^3)\Phi_2 = \Phi_2, \quad \rho_{\mathbf{3}}(T^3 ST^2 ST^3 S)\Phi_3 = \Phi_3. \tag{2.13}$$

We summarize that the GR mixing arises from the mismatch between the residual subgroups G_l and G_ν in the direct approach.

3 Golden Littlest Seesaw in A_5

3.1 Littlest Seesaw

The indirect model building approach [4] is an interesting alternative to the direct approach. In the indirect approach, the original flavor symmetry is completely broken in the neutrino sector, and the residual symmetry $Z_2 \times Z_2$ of the neutrino mass matrix arises accidentally. The basic idea of the indirect approach is to effectively promote the columns of the Dirac mass matrix to fields which transform as triplets under the flavour symmetry. We assume that the Dirac mass matrix can be written as $m_D = (a\Phi_{\text{atm}}, b\Phi_{\text{sol}}, c\Phi_{\text{dec}})$ where the columns are proportional to triplet Higgs scalar fields with particular vacuum alignments and a, b, c are three constants of proportionality. It is convenient to work in the basis where the right-handed neutrino mass matrix are diagonal with the mass eigenvalues equal to M_{atm} , M_{sol} and M_{dec} . Then the light neutrino mass matrix given by the seesaw formula is

$$m_\nu = a^2 \frac{\Phi_{\text{atm}}\Phi_{\text{atm}}^T}{M_{\text{atm}}} + b^2 \frac{\Phi_{\text{sol}}\Phi_{\text{sol}}^T}{M_{\text{sol}}} + c^2 \frac{\Phi_{\text{dec}}\Phi_{\text{dec}}^T}{M_{\text{dec}}}, \tag{3.1}$$

where we have dropped an overall minus sign which is physically irrelevant. In the case that the columns of the Dirac mass matrix are proportional to the columns of the GR matrix, $\Phi_{\text{atm}} \propto \Phi_3$, $\Phi_{\text{sol}} \propto \Phi_2$ and $\Phi_{\text{dec}} \propto \Phi_1$, the three columns of m_D would be mutually orthogonal,

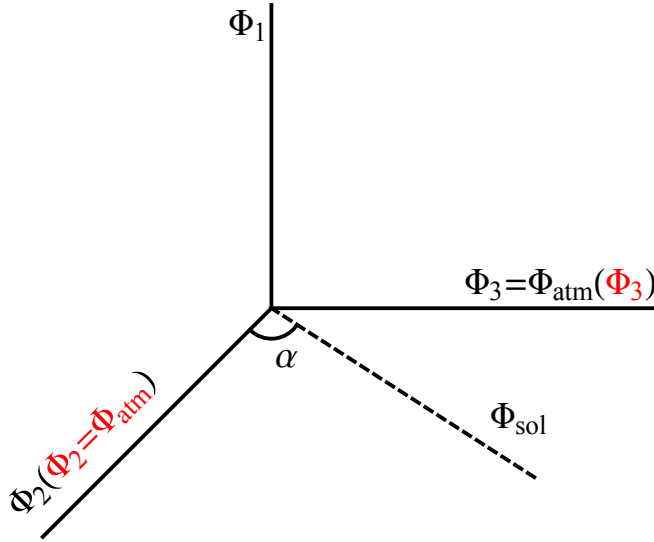


Figure 1: The vacuum alignment in the Littlest seesaw model. Φ_1 , Φ_2 and Φ_3 are the three columns of the golden ratio mixing matrix. The alignment vector Φ_{atm} is either Φ_2 or Φ_3 , and Φ_{sol} is a general vector orthogonal to Φ_1 .

as illustrated in figure 1. As a consequence, the resulting effective light Majorana mass matrix m_ν is form diagonalizable, and it is exactly diagonalized by the golden ratio mixing matrix. This scenario is referred to as form dominance [29]. In the limit of $M_{\text{dec}} \gg M_{\text{atm}}, M_{\text{sol}}$, as a good leading order approximation we could drop the last term and the model reduces to a two right-handed neutrino model, such that the lightest neutrino is massless.

The Littlest seesaw framework assumes that there are only two right-handed neutrinos to begin with, together with flavons which couple to them with particular vacuum alignments, leading to the columns of the Dirac mass matrix taking the above forms. Within the Littlest seesaw framework [15], we shall assume that both vacuum alignments Φ_{sol} and Φ_{atm} are orthogonal to Φ_1 , in order to preserve the first column of the mixing matrix. Then we shall choose Φ_{atm} to be either Φ_2 or Φ_3 , and take Φ_{sol} to be a general vector orthogonal to Φ_1 , as illustrated in figure 1. Later on we shall fix the alignment of Φ_{sol} by appealing to remnant symmetry, according to a generalisation of the direct approach, as discussed in the next subsection.

The Littlest seesaw is clearly a rather predictive framework which combines the two right-handed neutrino model with the indirect approach [9]. In this framework, two right-handed neutrinos N_R^{atm} and N_R^{sol} are introduced, and the third right-handed neutrino is assumed to be almost decoupled and irrelevant. N_R^{atm} dominantly contributes to the seesaw mechanism and is mainly responsible for the atmospheric neutrino mass m_3 . N_R^{sol} is sub-dominant and is mainly responsible for the solar neutrino mass m_2 while the lightest neutrino mass m_1 is zero in this limit. The Littlest seesaw model generally assumes three generations of left-handed neutrino fields $\nu_L = (\nu_e, \nu_\mu, \nu_\tau)$ transforms as a triplet of the flavor symmetry while both N_R^{atm} and N_R^{sol} are singlets. In the flavor basis where the charged lepton mass matrix is diagonal with real positive eigenvalues m_e, m_μ, m_τ and the right-handed neutrino Majorana mass matrix is also diagonal, by introducing appropriate auxiliary abelian symmetry, the generic Littlest seesaw Lagrangian can be written as

$$\mathcal{L} = -y_{\text{atm}} \bar{L} \cdot \phi_{\text{atm}} N_R^{\text{atm}} - y_{\text{sol}} \bar{L} \cdot \phi_{\text{sol}} N_R^{\text{sol}} - \frac{1}{2} M_{\text{atm}} \overline{(N_R^{\text{atm}})^c} N_R^{\text{atm}} - \frac{1}{2} M_{\text{sol}} \overline{(N_R^{\text{sol}})^c} N_R^{\text{sol}} + h.c., \quad (3.2)$$

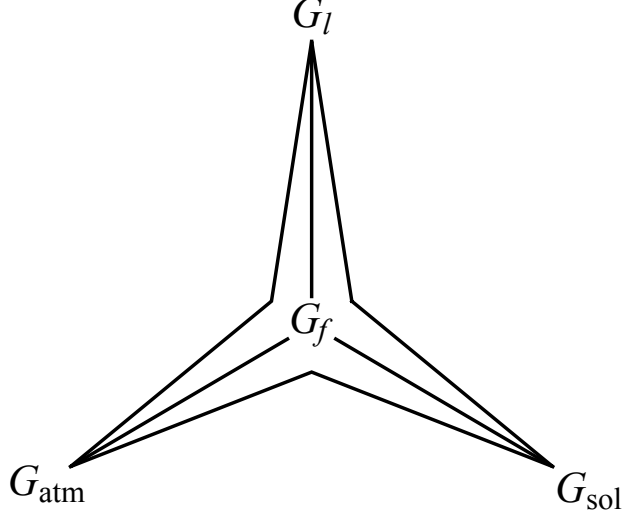


Figure 2: A sketch of the indirect model building approach, where the charged lepton preserves a residual subgroup G_l , and the neutrino vacuum alignments Φ_{atm} and Φ_{sol} are enforced by the residual symmetries G_{atm} and G_{sol} respectively.

where the flavons ϕ_{sol} and ϕ_{atm} can be either Higgs fields transforming as triplets under the flavour symmetry, or combinations of a single Higgs electroweak doublet together with triplet flavons. The fields L are the electroweak lepton doublets which are unified into a triplet representation of the flavor symmetry group. Then Φ_{atm} and Φ_{sol} in Eq. (3.1) arise from the vacuum expectation values (VEVs) of ϕ_{sol} and ϕ_{atm} respectively.

3.2 Indirect approach in A_5

The indirect approach is a further generalization of the direct approach. We assume that the A_5 group is broken to the abelian subgroup $G_l = Z_5^T$ in the charged lepton sector, the vacuum alignments Φ_{atm} and Φ_{sol} preserve different residual symmetries G_{atm} and G_{sol} respectively while the A_5 flavor symmetry is completely broken in the entire neutrino sector. The indirect approach is schematically illustrated in figure 2. In our GLS model, as stated above the alignment vector Φ_{sol} is orthogonal to Φ_1 , its most general form is

$$\Phi_{\text{sol}} \propto \left(\sqrt{2}, \phi - x, \phi + x \right)^T. \quad (3.3)$$

We find there are five possible values of x related to certain residual subgroups of A_5 ,

$$\begin{aligned} x = 0, & \quad G_{\text{sol}} = Z_2^{T^3 ST^2 ST^3}, \\ x = 2i\phi^2 \sin \frac{2\pi}{5}, & \quad G_{\text{sol}} = Z_3^{T^3 ST^2 S}, \\ x = -2i\phi^2 \sin \frac{2\pi}{5}, & \quad G_{\text{sol}} = Z_3^{ST^2 ST^3}, \\ x = -2i \sin \frac{\pi}{5}, & \quad G_{\text{sol}} = Z_5^{T^2 ST}, \\ x = 2i \sin \frac{\pi}{5}, & \quad G_{\text{sol}} = Z_5^{T ST^2}. \end{aligned} \quad (3.4)$$

Accordingly the vacuum alignment of the solar flavon ϕ_{sol} is:

$$\begin{aligned}
x = 0, \quad \Phi_{\text{sol}} &= \left(\sqrt{2}, \phi, \phi \right)^T, \\
x = 2i\phi^2 \sin \frac{2\pi}{5}, \quad \Phi_{\text{sol}} &= \left(\sqrt{2}, 2\phi^2 e^{-2i\pi/5}, 2\phi^2 e^{2i\pi/5} \right)^T, \\
x = -2i\phi^2 \sin \frac{2\pi}{5}, \quad \Phi_{\text{sol}} &= \left(\sqrt{2}, 2\phi^2 e^{2i\pi/5}, 2\phi^2 e^{-2i\pi/5} \right)^T, \\
x = -2i \sin \frac{\pi}{5}, \quad \Phi_{\text{sol}} &= \left(\sqrt{2}, 2e^{i\pi/5}, 2e^{-i\pi/5} \right)^T, \\
x = 2i \sin \frac{\pi}{5}, \quad \Phi_{\text{sol}} &= \left(\sqrt{2}, 2e^{-i\pi/5}, 2e^{i\pi/5} \right)^T.
\end{aligned} \tag{3.5}$$

In our framework, another alignment vector Φ_{atm} is assumed to be along the direction of Φ_3 or Φ_2 . In the following, we shall discuss the two cases one by one.

3.2.1 Golden Littlest seesaw with $\Phi_{\text{atm}} \propto \Phi_3$

In this case, the vacuum Φ_{atm} reads as

$$\Phi_{\text{atm}} \propto (0, -1, 1)^T, \tag{3.6}$$

which is invariant under the action of the $Z_2^{T^3 ST^2 ST^3 S}$ subgroup. Consequently the Dirac neutrino mass matrix M_D and the right-handed neutrino heavy Majorana mass matrix M_N are given by

$$M_D = \begin{pmatrix} 0 & \sqrt{2}b \\ -a & (\phi - x)b \\ a & (\phi + x)b \end{pmatrix}, \quad M_N = \begin{pmatrix} M_{\text{atm}} & 0 \\ 0 & M_{\text{sol}} \end{pmatrix} \tag{3.7}$$

Integrating out the right-handed neutrinos, the light effective Majorana neutrino mass matrix is approximately given by the seesaw formula

$$\begin{aligned}
m_\nu &= -M_D M_N^{-1} M_D^T \\
&= m_a \begin{pmatrix} 0 & 0 & 0 \\ 0 & 1 & -1 \\ 0 & -1 & 1 \end{pmatrix} + m_b e^{i\eta} \begin{pmatrix} 2 & \sqrt{2}(\phi - x) & \sqrt{2}(x + \phi) \\ \sqrt{2}(\phi - x) & (x - \phi)^2 & -x^2 + \phi + 1 \\ \sqrt{2}(x + \phi) & -x^2 + \phi + 1 & (x + \phi)^2 \end{pmatrix},
\end{aligned} \tag{3.8}$$

where $m_a = |a|^2/M_{\text{atm}}$, $m_b = |b|^2/M_{\text{sol}}$, the relative phase $\eta = \arg(b^2/a^2)$, and an overall phase of m_ν has been omitted. Therefore four parameters m_a , m_b , x and η describe both the neutrino flavor mixing and neutrino masses. One can check that neutrino mass matrix m_ν of Eq. (3.8) satisfies

$$m_\nu \begin{pmatrix} -\sqrt{\frac{\phi}{\sqrt{5}}} \\ \sqrt{\frac{1}{2\sqrt{5}\phi}} \\ \sqrt{\frac{1}{2\sqrt{5}\phi}} \end{pmatrix} = \begin{pmatrix} 0 \\ 0 \\ 0 \end{pmatrix}. \tag{3.9}$$

This implies that the column vector $(-\sqrt{\frac{\phi}{\sqrt{5}}}, \sqrt{\frac{1}{2\sqrt{5}\phi}}, \sqrt{\frac{1}{2\sqrt{5}\phi}})^T$ is an eigenvector of m_ν with a zero eigenvalue. As a result, the first column of the PMNS mixing matrix exactly coincides with the GR mixing pattern, and the corresponding light neutrino mass vanishes $m_1 = 0$.

In order to diagonalize the above neutrino mass matrix, we firstly perform a golden ratio transformation and obtain

$$m'_\nu = U_{GR}^T m_\nu U_{GR} = \begin{pmatrix} 0 & 0 & 0 \\ 0 & y & z \\ 0 & z & w \end{pmatrix} \quad (3.10)$$

where

$$\begin{aligned} y &= 2\sqrt{5}\phi m_b e^{i\eta}, \\ z &= 2x\sqrt{\phi+2} m_b e^{i\eta}, \\ w &= |w|e^{i\phi_w} = 2(m_a + x^2 m_b e^{i\eta}). \end{aligned} \quad (3.11)$$

The neutrino mass matrix m'_ν in Eq. (3.10) by diagonalized through the standard procedure, as shown in Ref. [30]. We have

$$U'^T_\nu m'_\nu U'_\nu = \text{diag}(0, m_2, m_3), \quad (3.12)$$

where the unitary matrix U'_ν can be written as

$$U'_\nu = \begin{pmatrix} 1 & 0 & 0 \\ 0 & \cos\theta e^{i(\psi+\rho)/2} & \sin\theta e^{i(\psi+\sigma)/2} \\ 0 & -\sin\theta e^{i(-\psi+\rho)/2} & \cos\theta e^{i(-\psi+\sigma)/2} \end{pmatrix}. \quad (3.13)$$

We find the light neutrino masses $m_{2,3}$ are

$$\begin{aligned} m_2^2 &= \frac{1}{2} \left[|y|^2 + |w|^2 + 2|z|^2 - \frac{|w|^2 - |y|^2}{\cos 2\theta} \right], \\ m_3^2 &= \frac{1}{2} \left[|y|^2 + |w|^2 + 2|z|^2 + \frac{|w|^2 - |y|^2}{\cos 2\theta} \right] \end{aligned} \quad (3.14)$$

The rotation angle θ is determined to be

$$\begin{aligned} \sin 2\theta &= \frac{-2iz e^{-i\eta} \sqrt{|y|^2 + |w|^2 - 2|y||w| \cos(\phi_w - \eta)}}{\sqrt{(|w|^2 - |y|^2)^2 + 4|z|^2 [|y|^2 + |w|^2 - 2|y||w| \cos(\phi_w - \eta)]}}, \\ \cos 2\theta &= \frac{|w|^2 - |y|^2}{\sqrt{(|w|^2 - |y|^2)^2 + 4|z|^2 [|y|^2 + |w|^2 - 2|y||w| \cos(\phi_w - \eta)]}}. \end{aligned} \quad (3.15)$$

The phases ψ , ρ and σ are given by

$$\begin{aligned} \sin \psi &= \frac{|y| - |w| \cos(\phi_w - \eta)}{\sqrt{|y|^2 + |w|^2 - 2|y||w| \cos(\phi_w - \eta)}}, \quad \cos \psi = \frac{|w| \sin(\phi_w - \eta)}{\sqrt{|y|^2 + |w|^2 - 2|y||w| \cos(\phi_w - \eta)}}, \\ \sin \rho &= -\frac{(m_2^2 - |z|^2) \cos \eta - |y||w| \cos \phi_w}{m_2 \sqrt{|y|^2 + |w|^2 - 2|y||w| \cos(\phi_w - \eta)}}, \quad \cos \rho = \frac{-(m_2^2 - |z|^2) \sin \eta + |y||w| \sin \phi_w}{m_2 \sqrt{|y|^2 + |w|^2 - 2|y||w| \cos(\phi_w - \eta)}}, \\ \sin \sigma &= -\frac{(m_3^2 - |z|^2) \cos \eta - |y||w| \cos \phi_w}{m_3 \sqrt{|y|^2 + |w|^2 - 2|y||w| \cos(\phi_w - \eta)}}, \quad \cos \sigma = \frac{-(m_3^2 - |z|^2) \sin \eta + |y||w| \sin \phi_w}{m_3 \sqrt{|y|^2 + |w|^2 - 2|y||w| \cos(\phi_w - \eta)}}. \end{aligned} \quad (3.16)$$

Thus the lepton mixing matrix is determined to be

$$U = U_{GR} U'_\nu = \sqrt{\frac{1}{2\sqrt{5}\phi}} \begin{pmatrix} -\sqrt{2}\phi & \sqrt{2}\cos\theta & \sqrt{2}e^{i\psi}\sin\theta \\ 1 & \phi\cos\theta + \sqrt{\phi+2}\sin\theta e^{-i\psi} & \phi\sin\theta e^{i\psi} - \sqrt{\phi+2}\cos\theta \\ 1 & \phi\cos\theta - \sqrt{\phi+2}\sin\theta e^{-i\psi} & \phi\sin\theta e^{i\psi} + \sqrt{\phi+2}\cos\theta \end{pmatrix} P_\nu, \quad (3.17)$$

with

$$P_\nu = \text{diag}(1, e^{i(\psi+\rho)/2}, e^{i(-\psi+\sigma)/2}). \quad (3.18)$$

The most general leptonic mixing matrix in the two right-handed neutrino model can be parameterized as

$$U = \begin{pmatrix} c_{12}c_{13} & s_{12}c_{13} & s_{13}e^{-i\delta_{CP}} \\ -s_{12}c_{23} - c_{12}s_{13}s_{23}e^{i\delta_{CP}} & c_{12}c_{23} - s_{12}s_{13}s_{23}e^{i\delta_{CP}} & c_{13}s_{23} \\ s_{12}s_{23} - c_{12}s_{13}c_{23}e^{i\delta_{CP}} & -c_{12}s_{23} - s_{12}s_{13}c_{23}e^{i\delta_{CP}} & c_{13}c_{23} \end{pmatrix} \text{diag}(1, e^{i\frac{\beta}{2}}, 1), \quad (3.19)$$

where $c_{ij} \equiv \cos \theta_{ij}$, $s_{ij} \equiv \sin \theta_{ij}$, δ_{CP} is the Dirac CP violation phase and β is the Majorana CP phase. Note that a second Majorana phase is needed if the lightest neutrino is not massless. Then we can extract the expressions for the lepton mixing angles as follows

$$\begin{aligned} \sin^2 \theta_{13} &= \frac{\sin^2 \theta}{\sqrt{5}\phi}, & \sin^2 \theta_{12} &= \frac{\cos^2 \theta}{\sqrt{5}\phi - \sin^2 \theta}, \\ \sin^2 \theta_{23} &= \frac{1}{2} - \frac{\sqrt{3+4\phi} \sin 2\theta \cos \psi}{2(\sqrt{5}\phi - \sin^2 \theta)}. \end{aligned} \quad (3.20)$$

Eliminating the free parameter θ , we see that a sum rule between the solar mixing angle θ_{12} and the reactor mixing angle θ_{13} is satisfied,

$$\cos^2 \theta_{12} \cos^2 \theta_{13} = \frac{\phi}{\sqrt{5}}. \quad (3.21)$$

Using the best fit value of $\sin^2 \theta_{13} = 0.0215$, we find for the solar mixing angle

$$\sin^2 \theta_{12} \simeq 0.261, \quad (3.22)$$

which is within the 3σ region [1]. As regards the CP violation, two weak basis invariants J_{CP} [31] and I_1 [32] associated with the CP phases δ_{CP} and β respectively can be defined,

$$\begin{aligned} J_{CP} &= \Im(U_{11}U_{33}U_{13}^*U_{31}^*) = \frac{1}{8} \sin 2\theta_{12} \sin 2\theta_{13} \sin 2\theta_{23} \cos \theta_{13} \sin \delta_{CP}, \\ I_1 &= \Im(U_{12}^2U_{13}^{*2}) = \frac{1}{4} \sin^2 \theta_{12} \sin^2 2\theta_{13} \sin(\beta + 2\delta_{CP}). \end{aligned} \quad (3.23)$$

For the mixing pattern in Eq. (3.19), these CP invariants turn out to be

$$J_{CP} = \frac{\sin 2\theta \sin \psi}{4\sqrt{5}(\phi + 2)}, \quad I_1 = \frac{1}{20\phi^2} \sin^2 2\theta \sin(\rho - \sigma). \quad (3.24)$$

Since J_{CP} and all the three mixing angles depend on only two parameters θ and ψ , we can derive the following sum rule among the Dirac CP phase δ_{CP} and mixing angles

$$\cos \delta_{CP} = \frac{(\phi + 2)(1 + \sin^2 \theta_{13}) - 5 \cos^2 \theta_{13}}{2\sqrt{(\phi + 2)(5 \cos^2 \theta_{13} - \phi - 2)}} \csc \theta_{13} \cot 2\theta_{23}. \quad (3.25)$$

For maximal atmospheric mixing angle $\theta_{23} = \pi/4$, this sum rule predicts $\cos \delta_{CP} = 0$ which corresponds to maximal CP violation $\delta_{CP} = \pm\pi/2$. The mixing angles, CP phases and mass ratio m_2/m_3 depend on the x , η and $r \equiv m_b/m_a$ while m_2 and m_3 depend on all the

four input parameters x , η , m_a and m_b . By comprehensively scanning over the parameter space of η and r , we find that the experimental data on the mixing angles and mass squared splittings can be accommodated only for the values of $x = \pm 2i\phi^2 \sin \frac{2\pi}{5}$. In table 2 we present the predictions for the mixing angles and CP violation phases for some benchmark values of the parameters η and r . It is remarkable that both atmospheric mixing angle and Dirac phase are maximal for $\eta = 0$, all the mixing angles and mass ratio m_2^2/m_3^2 lie in the experimentally preferred 3σ ranges except that the reactor angle θ_{13} is a bit smaller. This tiny discrepancy is expected to be easily resolved in an explicit model with small corrections or by the renormalization group corrections [33]. Notice that the same predictions for the mixing angles and maximal δ_{CP} can be obtained from the approach of combining A_5 flavor symmetry with generalized CP [22,27,28], but we have additional prediction for the neutrino masses here even if the CP symmetry is not introduced in the present context. We can check that the neutrino mass matrix m_ν in Eq. (3.8) has the following symmetry properties

$$\begin{aligned} m_\nu(\eta, x = \pm 2i\phi^2 \sin 2\pi/5) &= P_{23}^T m_\nu(\eta, x = \mp 2i\phi^2 \sin 2\pi/5) P_{23}, \\ m_\nu(\eta, x = \pm 2i\phi^2 \sin 2\pi/5) &= m_\nu^*(-\eta, x = \mp 2i\phi^2 \sin 2\pi/5), \end{aligned} \quad (3.26)$$

with

$$P_{23} = \begin{pmatrix} 1 & 0 & 0 \\ 0 & 0 & 1 \\ 0 & 1 & 0 \end{pmatrix}. \quad (3.27)$$

As a consequence, the same reactor and solar mixing angles are obtained for $x = 2i\phi^2 \sin \frac{2\pi}{5}$ and $x = -2i\phi^2 \sin \frac{2\pi}{5}$, while the atmospheric angle changes from θ_{23} to $\pi/2 - \theta_{23}$ and the Dirac phase changes from δ_{CP} to $\pi + \delta_{CP}$. Moreover, all the lepton mixing angles are kept intact and the signs of all CP violation phases are reversed under the transformation $x \rightarrow -x$ and $\eta \rightarrow -\eta$. For the fixed value of $x = \pm 2i\phi^2 \sin \frac{2\pi}{5}$, all the mixing angles, CP phases and mass ratio m_2^2/m_3^2 are fully determined by r and η , and the correct neutrino mass m_2 can be achieved for certain values of m_b . We show how these mixing parameters vary in the plane η versus r in figure 3. It can be seen that the measured values of the mixing angles and the neutrino masses can be accommodated for certain choices of η and r .

3.2.2 Golden Littlest seesaw with $\Phi_{\text{atm}} \propto \Phi_2$

Similar to previous case, the most general form of the solar vacuum Φ_{sol} is given by Eq. (4.8), and the atmospheric alignment vector takes the form

$$\Phi_{\text{atm}} \propto \left(\sqrt{2}, \phi, \phi \right)^T, \quad (3.28)$$

which preserves the residual symmetry $G_{\text{atm}} = Z_2^{T^3 ST^2 ST^3}$. Subsequently we can read out the Dirac neutrino mass matrix M_D and the right-handed neutrino mass matrix M_N as

$$M_D = \begin{pmatrix} \sqrt{2}a & \sqrt{2}b \\ \phi a & (\phi - x)b \\ \phi a & (\phi + x)b \end{pmatrix}, \quad M_N = \begin{pmatrix} M_{\text{atm}} & 0 \\ 0 & M_{\text{sol}} \end{pmatrix}, \quad (3.29)$$

which leads to the following low energy effective Majorana neutrino mass matrix

$$m_\nu = m_a \begin{pmatrix} 2 & \sqrt{2}\phi & \sqrt{2}\phi \\ \sqrt{2}\phi & \phi + 1 & \phi + 1 \\ \sqrt{2}\phi & \phi + 1 & \phi + 1 \end{pmatrix} + m_b e^{i\eta} \begin{pmatrix} 2 & \sqrt{2}(\phi - x) & \sqrt{2}(x + \phi) \\ \sqrt{2}(\phi - x) & (x - \phi)^2 & -x^2 + \phi + 1 \\ \sqrt{2}(x + \phi) & -x^2 + \phi + 1 & (x + \phi)^2 \end{pmatrix}, \quad (3.30)$$

η	r	x	$\sin^2 \theta_{13}$	$\sin^2 \theta_{12}$	$\sin^2 \theta_{23}$	δ_{CP}/π	β/π	m_2^2/m_3^2
0	0.0177	$\pm 2i\phi^2 \sin \frac{2\pi}{5}$	0.0164	0.264	0.5	∓ 0.5	0	0.0309
$\pm \frac{\pi}{11}$	0.0185	$\pm 2i\phi^2 \sin \frac{2\pi}{5}$	0.0174	0.264	0.614	∓ 0.331	∓ 0.210	0.0302
$\pm \frac{\pi}{11}$	0.0185	$\mp 2i\phi^2 \sin \frac{2\pi}{5}$	0.0175	0.264	0.385	± 0.670	∓ 0.211	0.0304
$\pm \frac{\pi}{12}$	0.0183	$\pm 2i\phi^2 \sin \frac{2\pi}{5}$	0.0172	0.264	0.605	∓ 0.345	∓ 0.192	0.0303
$\pm \frac{\pi}{12}$	0.0184	$\mp 2i\phi^2 \sin \frac{2\pi}{5}$	0.0173	0.264	0.394	± 0.655	∓ 0.192	0.0305
$\pm \frac{\pi}{13}$	0.0182	$\pm 2i\phi^2 \sin \frac{2\pi}{5}$	0.0171	0.264	0.597	∓ 0.357	∓ 0.176	0.0304
$\pm \frac{\pi}{13}$	0.0183	$\mp 2i\phi^2 \sin \frac{2\pi}{5}$	0.0172	0.264	0.402	± 0.643	∓ 0.177	0.0306
$\pm \frac{\pi}{14}$	0.0182	$\pm 2i\phi^2 \sin \frac{2\pi}{5}$	0.0170	0.264	0.591	∓ 0.368	∓ 0.163	0.0304
$\pm \frac{\pi}{14}$	0.0182	$\mp 2i\phi^2 \sin \frac{2\pi}{5}$	0.0171	0.264	0.409	± 0.632	∓ 0.164	0.0307
$\pm \frac{\pi}{15}$	0.0181	$\pm 2i\phi^2 \sin \frac{2\pi}{5}$	0.0169	0.264	0.585	∓ 0.377	∓ 0.152	0.0305
$\pm \frac{\pi}{15}$	0.0181	$\mp 2i\phi^2 \sin \frac{2\pi}{5}$	0.0170	0.264	0.415	± 0.623	∓ 0.152	0.0307
$\pm \frac{\pi}{16}$	0.0180	$\pm 2i\phi^2 \sin \frac{2\pi}{5}$	0.0168	0.264	0.580	∓ 0.385	∓ 0.142	0.0305
$\pm \frac{\pi}{16}$	0.0181	$\mp 2i\phi^2 \sin \frac{2\pi}{5}$	0.0169	0.264	0.420	± 0.616	∓ 0.142	0.0308
$\pm \frac{\pi}{17}$	0.0180	$\pm 2i\phi^2 \sin \frac{2\pi}{5}$	0.0168	0.264	0.575	∓ 0.391	∓ 0.134	0.0306
$\pm \frac{\pi}{17}$	0.0180	$\mp 2i\phi^2 \sin \frac{2\pi}{5}$	0.0169	0.264	0.425	± 0.609	∓ 0.134	0.0308
$\pm \frac{\pi}{18}$	0.0180	$\pm 2i\phi^2 \sin \frac{2\pi}{5}$	0.0167	0.264	0.571	∓ 0.398	∓ 0.126	0.0306
$\pm \frac{\pi}{18}$	0.0180	$\mp 2i\phi^2 \sin \frac{2\pi}{5}$	0.0168	0.264	0.429	± 0.603	∓ 0.126	0.0308
$\pm \frac{\pi}{19}$	0.0179	$\pm 2i\phi^2 \sin \frac{2\pi}{5}$	0.0167	0.264	0.567	∓ 0.403	∓ 0.119	0.0306
$\pm \frac{\pi}{19}$	0.0180	$\mp 2i\phi^2 \sin \frac{2\pi}{5}$	0.0168	0.264	0.432	± 0.597	∓ 0.119	0.0308
$\pm \frac{\pi}{20}$	0.0179	$\pm 2i\phi^2 \sin \frac{2\pi}{5}$	0.0167	0.264	0.564	∓ 0.408	∓ 0.113	0.0306
$\pm \frac{\pi}{20}$	0.0179	$\mp 2i\phi^2 \sin \frac{2\pi}{5}$	0.0167	0.264	0.436	± 0.592	∓ 0.113	0.0308
$\pm \frac{\pi}{21}$	0.0179	$\pm 2i\phi^2 \sin \frac{2\pi}{5}$	0.0166	0.264	0.561	∓ 0.412	∓ 0.108	0.0306
$\pm \frac{\pi}{21}$	0.0179	$\mp 2i\phi^2 \sin \frac{2\pi}{5}$	0.0167	0.264	0.439	± 0.588	∓ 0.108	0.0308
$\pm \frac{\pi}{22}$	0.0179	$\pm 2i\phi^2 \sin \frac{2\pi}{5}$	0.0166	0.264	0.558	∓ 0.416	∓ 0.103	0.0307
$\pm \frac{\pi}{22}$	0.0179	$\mp 2i\phi^2 \sin \frac{2\pi}{5}$	0.0167	0.264	0.442	± 0.584	∓ 0.103	0.0309
$\pm \frac{\pi}{23}$	0.0179	$\pm 2i\phi^2 \sin \frac{2\pi}{5}$	0.0166	0.264	0.556	∓ 0.420	∓ 0.0982	0.0307
$\pm \frac{\pi}{23}$	0.0179	$\mp 2i\phi^2 \sin \frac{2\pi}{5}$	0.0167	0.264	0.444	± 0.580	∓ 0.0983	0.0309
$\pm \frac{2\pi}{23}$	0.0184	$\pm 2i\phi^2 \sin \frac{2\pi}{5}$	0.0173	0.264	0.610	∓ 0.338	∓ 0.201	0.0302
$\pm \frac{2\pi}{23}$	0.0184	$\mp 2i\phi^2 \sin \frac{2\pi}{5}$	0.0174	0.264	0.390	± 0.662	∓ 0.201	0.0305

Table 2: Predictions for all the lepton mixing angles, CP violation phases and m_2^2/m_3^2 in the golden Littlest seesaw with $\Phi_{\text{atm}} \propto \Phi_3$. Here we choose many benchmark values for the parameters η and r .

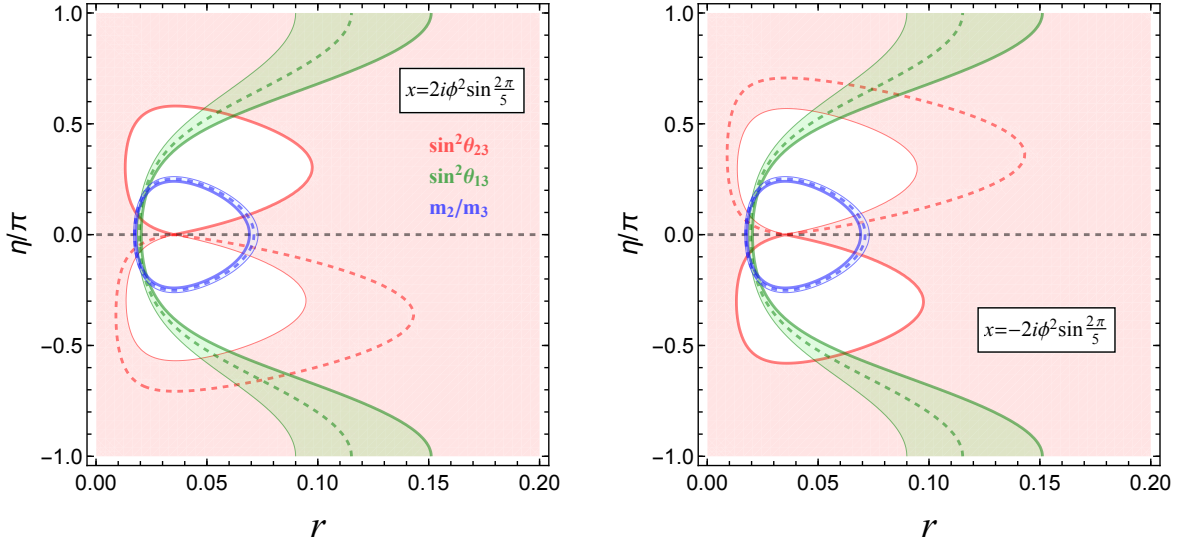


Figure 3: Contour plots of $\sin^2 \theta_{13}$, $\sin^2 \theta_{23}$ and m_2/m_3 in the $\eta - r$ plane for the golden Littlest seesaw with $\Phi_{\text{atm}} \propto \Phi_3$. Here we take $x = 2i\phi^2 \sin(2\pi/5)$ and $x = -2i\phi^2 \sin(2\pi/5)$ for which the solar vacuum alignment Φ_{sol} preserves the residual symmetry $G_{\text{sol}} = Z_3^{T^3} S T^2 S$ and $G_{\text{sol}} = Z_3^{S T^2} S T^3$ respectively. The 3σ upper (lower) bounds of the lepton mixing angles are labelled with thick (thin) solid curves, and the dashed contour lines represent the corresponding best fit values. The 3σ ranges as well as the best fit values of the mixing angles are adapted from [1]. The black contour line refers to maximal atmospheric mixing angle with $\sin^2 \theta_{23} = 0.5$.

with $m_a = |a|^2/M_{\text{atm}}$, $m_b = |b|^2/M_{\text{sol}}$ and $\eta = \arg(b^2/a^2)$. This model is rather predictive since only four parameters m_a , m_b , x and η can describe the entire neutrino sector. The symmetry relations in Eq. (3.26) are also satisfied in this case. The neutrino mass matrix in Eq. (3.30) can be block diagonalized by the GR mixing matrix,

$$m'_\nu = U_{GR}^T m_\nu U_{GR} = \begin{pmatrix} 0 & 0 & 0 \\ 0 & y & z \\ 0 & z & w \end{pmatrix}, \quad (3.31)$$

where

$$\begin{aligned} y &= |y|e^{i\phi_y} = 2\sqrt{5}\phi(m_a + m_b e^{i\eta}), \\ z &= 2x\sqrt{\phi+2}m_b e^{i\eta}, \\ w &= 2x^2 m_b e^{i\eta}. \end{aligned} \quad (3.32)$$

Furthermore, m'_ν can be put into diagonal form by performing another unitary transformation

$$U'^T m'_\nu U' = \text{diag}(0, m_2, m_3), \quad (3.33)$$

with

$$U' = \begin{pmatrix} 1 & 0 & 0 \\ 0 & \cos \theta e^{i(\psi+\rho)/2} & \sin \theta e^{i(\psi+\sigma)/2} \\ 0 & -\sin \theta e^{i(-\psi+\rho)/2} & \cos \theta e^{i(-\psi+\sigma)/2} \end{pmatrix}, \quad (3.34)$$

where the parameters θ , ψ , ρ and σ are determined in terms of x , y , z defined in Eq. (3.32),

$$\begin{aligned}
\sin 2\theta &= \frac{-2iz e^{-i\eta} \sqrt{|y|^2 + |w|^2 - 2|y||w| \cos(\phi_y - \eta)}}{\sqrt{(|w|^2 - |y|^2)^2 + 4|z|^2 [|y|^2 + |w|^2 - 2|y||w| \cos(\phi_y - \eta)]}}, \\
\cos 2\theta &= \frac{|w|^2 - |y|^2}{\sqrt{(|w|^2 - |y|^2)^2 + 4|z|^2 [|y|^2 + |w|^2 - 2|y||w| \cos(\phi_y - \eta)]}}, \\
\sin \psi &= \frac{|y| \cos(\phi_y - \eta) - |w|}{\sqrt{|y|^2 + |w|^2 - 2|y||w| \cos(\phi_y - \eta)}}, \\
\cos \psi &= \frac{|y| \sin(\phi_y - \eta)}{\sqrt{|y|^2 + |w|^2 - 2|y||w| \cos(\phi_y - \eta)}}, \\
\sin \rho &= -\frac{(m_2^2 - |z|^2) \cos \eta - |y||w| \cos \phi_y}{m_2 \sqrt{|y|^2 + |w|^2 - 2|y||w| \cos(\phi_y - \eta)}}, \\
\cos \rho &= \frac{-(m_2^2 - |z|^2) \sin \eta + |y||w| \sin \phi_y}{m_2 \sqrt{|y|^2 + |w|^2 - 2|y||w| \cos(\phi_y - \eta)}}, \\
\sin \sigma &= -\frac{(m_3^2 - |z|^2) \cos \eta - |y||w| \cos \phi_y}{m_3 \sqrt{|y|^2 + |w|^2 - 2|y||w| \cos(\phi_y - \eta)}}, \\
\cos \sigma &= \frac{-(m_3^2 - |z|^2) \sin \eta + |y||w| \sin \phi_y}{m_3 \sqrt{|y|^2 + |w|^2 - 2|y||w| \cos(\phi_y - \eta)}}. \tag{3.35}
\end{aligned}$$

The exact expressions for the neutrino masses are given by

$$\begin{aligned}
m_1^2 &= 0, \\
m_2^2 &= \frac{1}{2} \left[|y|^2 + |w|^2 + 2|z|^2 - \frac{|w|^2 - |y|^2}{\cos 2\theta} \right], \\
m_3^2 &= \frac{1}{2} \left[|y|^2 + |w|^2 + 2|z|^2 + \frac{|w|^2 - |y|^2}{\cos 2\theta} \right] \tag{3.36}
\end{aligned}$$

Given that the charged lepton mass matrix is diagonal due to the Z_5^T residual symmetry, the PMNS mixing matrix is of the form

$$U = U_{GR} U' = \sqrt{\frac{\phi - 1}{2\sqrt{5}}} \begin{pmatrix} -\sqrt{2}\phi & \sqrt{2} \cos \theta & \sqrt{2} e^{i\psi} \sin \theta \\ 1 & \phi \cos \theta + \sqrt{\phi + 2} \sin \theta e^{-i\psi} & \phi \sin \theta e^{i\psi} - \sqrt{\phi + 2} \cos \theta \\ 1 & \phi \cos \theta - \sqrt{\phi + 2} \sin \theta e^{-i\psi} & \phi \sin \theta e^{i\psi} + \sqrt{\phi + 2} \cos \theta \end{pmatrix} P_\nu, \tag{3.37}$$

with

$$P_\nu = \text{diag}(1, e^{i(\psi+\rho)/2}, e^{i(-\psi+\sigma)/2}). \tag{3.38}$$

Obviously the first column of the mixing matrix is fixed to be that of the GR mixing matrix. The lepton mixing matrix U is identical with the one in Eq. (3.17). Hence all the mixing angles and CP invariants are predicted to have the same form as those of Eq. (3.20) and Eq. (3.24) respectively, but their dependence on the input parameters m_a , m_b , η and x are different. The sum rules in Eq. (3.21) and Eq. (3.25) are satisfied as well. Detailed numerical analyses show that accordance with experimental data can be achieved for certain values of $r = m_b/m_a$ and η in the case of $x = \pm 2i\phi^2 \sin \frac{2\pi}{5}$, and the corresponding benchmark numerical results are listed in table 3. The most interesting point is $\eta = \pi$ which predicts

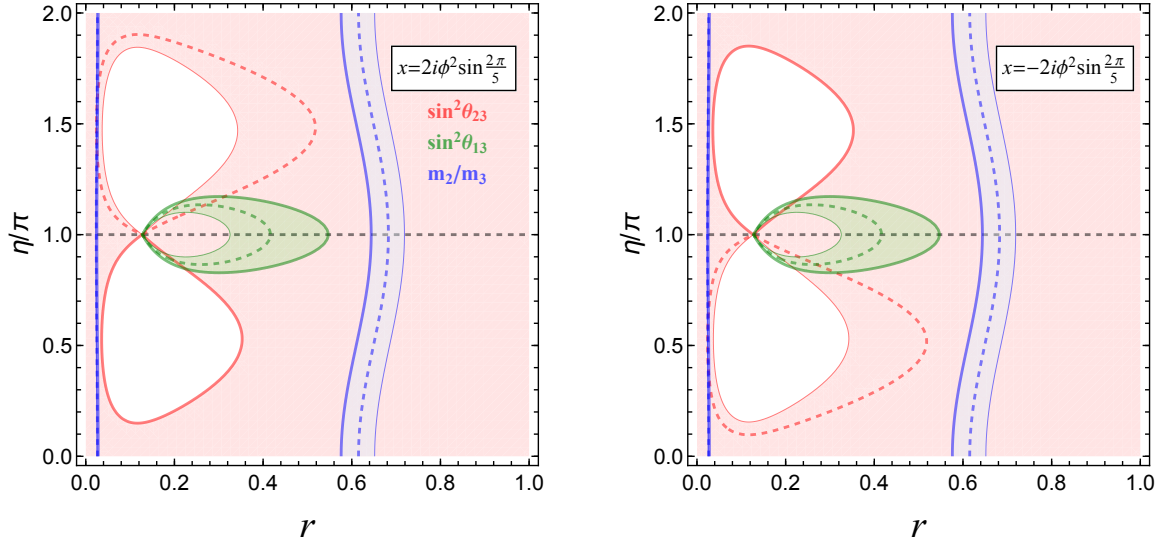


Figure 4: Contour plots of $\sin^2 \theta_{13}$, $\sin^2 \theta_{23}$ and m_2/m_3 in the $\eta - r$ plane for the golden Littlest seesaw with $\Phi_{\text{atm}} \propto \Phi_2$. Here we take $x = 2i\phi^2 \sin(2\pi/5)$ and $x = -2i\phi^2 \sin(2\pi/5)$ for which the solar vacuum alignment Φ_{sol} preserves the residual symmetry $G_{\text{sol}} = Z_3^{T^3 ST^2 S}$ and $G_{\text{sol}} = Z_3^{ST^2 ST^3}$ respectively. The 3σ upper (lower) bounds of the lepton mixing angles are labelled with thick (thin) solid curves, and the dashed contour lines represent the corresponding best fit values. The 3σ ranges as well as the best fit values of the mixing angles are adapted from [1]. The black contour line refers to maximal atmospheric mixing angle with $\sin^2 \theta_{23} = 0.5$.

maximal atmospheric mixing and a maximal Dirac phase. The realistic values of $\sin^2 \theta_{12}$ and m_2^2/m_3^2 can be obtained for $r = 1.486$ while the reactor angle is slightly a bit larger. This mixing pattern for $\eta = \pi$ can also be obtained from A_5 flavor symmetry and CP in the semidirect approach [22, 27, 28], the additional bonus in GLS is the prediction for neutrino masses. As discussed in above, all the mixing parameters as well as mass ratio m_2/m_3 depend only on η and r , this dependence is shown in figure 4.

If we further take into account the contribution of the third almost decoupled right-handed neutrino of mass M_{dec} , for example for the case of $\Phi_{\text{dec}} \propto \Phi_1$, the last term of Eq. (3.1) would contribute to the lightest neutrino mass $m_1 = c^2/M_{\text{dec}}$, while the neutrino mixing angles, CP violating phases and the other two neutrino masses are not changed. From figure 5, we can see that better agreement with experimental data can be achieved. The viable regions for $\sin^2 \theta_{13}$, $\sin^2 \theta_{23}$ and m_2/m_3 can overlap with each other.

η	r	x	$\sin^2 \theta_{13}$	$\sin^2 \theta_{12}$	$\sin^2 \theta_{23}$	δ_{CP}/π	β/π	m_2^2/m_3^2
π	0.675	$\pm 2i\phi^2 \sin \frac{2\pi}{5}$	0.0257	0.257	± 0.5	0.5	0	0.0294
$\pm \frac{4\pi}{5}$	0.670	$\pm 2i\phi^2 \sin \frac{2\pi}{5}$	0.0282	0.255	0.535	± 0.465	∓ 0.203	0.0293
$\pm \frac{4\pi}{5}$	0.669	$\mp 2i\phi^2 \sin \frac{2\pi}{5}$	0.0282	0.255	0.465	∓ 0.536	∓ 0.203	0.0294
$\pm \frac{5\pi}{6}$	0.671	$\pm 2i\phi^2 \sin \frac{2\pi}{5}$	0.0275	0.256	0.529	± 0.469	∓ 0.169	0.0294
$\pm \frac{5\pi}{6}$	0.67	$\mp 2i\phi^2 \sin \frac{2\pi}{5}$	0.0274	0.256	0.47	∓ 0.531	∓ 0.169	0.0295
$\pm \frac{6\pi}{7}$	0.672	$\pm 2i\phi^2 \sin \frac{2\pi}{5}$	0.027	0.256	0.526	± 0.473	∓ 0.145	0.0294
$\pm \frac{6\pi}{7}$	0.671	$\mp 2i\phi^2 \sin \frac{2\pi}{5}$	0.027	0.256	0.474	∓ 0.527	∓ 0.145	0.0295
$\pm \frac{7\pi}{8}$	0.673	$\pm 2i\phi^2 \sin \frac{2\pi}{5}$	0.0267	0.257	0.523	± 0.476	∓ 0.127	0.0294
$\pm \frac{7\pi}{8}$	0.672	$\mp 2i\phi^2 \sin \frac{2\pi}{5}$	0.0267	0.257	0.477	∓ 0.524	∓ 0.127	0.0295
$\pm \frac{8\pi}{9}$	0.674	$\pm 2i\phi^2 \sin \frac{2\pi}{5}$	0.0265	0.257	0.52	± 0.479	∓ 0.113	0.0294
$\pm \frac{8\pi}{9}$	0.673	$\mp 2i\phi^2 \sin \frac{2\pi}{5}$	0.0265	0.257	0.48	∓ 0.521	∓ 0.113	0.0295
$\pm \frac{9\pi}{10}$	0.674	$\pm 2i\phi^2 \sin \frac{2\pi}{5}$	0.0264	0.257	0.518	± 0.481	∓ 0.101	0.0294
$\pm \frac{9\pi}{10}$	0.673	$\mp 2i\phi^2 \sin \frac{2\pi}{5}$	0.0263	0.257	0.482	∓ 0.519	∓ 0.101	0.0295
$\pm \frac{10\pi}{11}$	0.674	$\pm 2i\phi^2 \sin \frac{2\pi}{5}$	0.0262	0.257	0.517	± 0.482	∓ 0.0922	0.0294
$\pm \frac{10\pi}{11}$	0.674	$\mp 2i\phi^2 \sin \frac{2\pi}{5}$	0.0262	0.257	0.483	∓ 0.518	∓ 0.0922	0.0294
$\pm \frac{11\pi}{12}$	0.674	$\pm 2i\phi^2 \sin \frac{2\pi}{5}$	0.0262	0.257	0.515	± 0.484	∓ 0.0845	0.0294
$\pm \frac{11\pi}{12}$	0.674	$\mp 2i\phi^2 \sin \frac{2\pi}{5}$	0.0262	0.257	0.485	∓ 0.516	∓ 0.0845	0.0294
$\pm \frac{12\pi}{13}$	0.675	$\pm 2i\phi^2 \sin \frac{2\pi}{5}$	0.0261	0.257	0.514	± 0.485	∓ 0.078	0.0294
$\pm \frac{12\pi}{13}$	0.674	$\mp 2i\phi^2 \sin \frac{2\pi}{5}$	0.0261	0.257	0.486	∓ 0.515	∓ 0.078	0.0294
$\pm \frac{13\pi}{14}$	0.675	$\pm 2i\phi^2 \sin \frac{2\pi}{5}$	0.0260	0.257	0.513	± 0.486	∓ 0.0724	0.0294
$\pm \frac{13\pi}{14}$	0.674	$\mp 2i\phi^2 \sin \frac{2\pi}{5}$	0.0260	0.257	0.487	∓ 0.514	∓ 0.0724	0.0294
$\pm \frac{13\pi}{15}$	0.673	$\pm 2i\phi^2 \sin \frac{2\pi}{5}$	0.0268	0.256	0.524	± 0.475	∓ 0.135	0.0294
$\pm \frac{13\pi}{15}$	0.672	$\mp 2i\phi^2 \sin \frac{2\pi}{5}$	0.0268	0.256	0.476	∓ 0.525	∓ 0.135	0.0295
$\pm \frac{14\pi}{15}$	0.675	$\pm 2i\phi^2 \sin \frac{2\pi}{5}$	0.0260	0.257	0.512	± 0.487	∓ 0.0676	0.0294
$\pm \frac{14\pi}{15}$	0.674	$\mp 2i\phi^2 \sin \frac{2\pi}{5}$	0.0260	0.257	0.488	∓ 0.513	∓ 0.0676	0.0294

Table 3: Benchmark numerical results in the golden Littlest seesaw for the case of $\Phi_{\text{atm}} \propto \Phi_2$ and $x = \pm 2i\phi^2 \sin(2\pi/5)$.

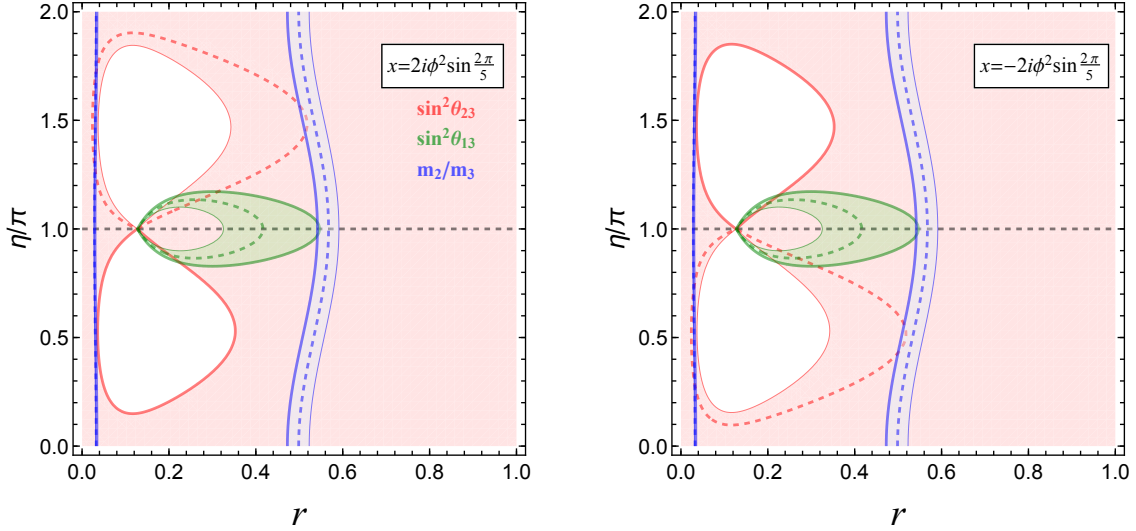


Figure 5: Contour plots of $\sin^2 \theta_{13}$, $\sin^2 \theta_{23}$ and m_2/m_3 in the $\eta - r$ plane for the golden Littlest seesaw with $\Phi_{\text{atm}} \propto \Phi_2$. As an example, we assume that the decoupled alignment $\Phi_{\text{dec}} \propto \Phi_1$ which gives rise to $m_1 = 6 \times 10^{-3} \text{eV}$.

4 Alternative Golden Littlest Seesaw in A_5

In the direct approach, if the A_5 flavor symmetry is broken down to Klein subgroups in both the neutrino and charged lepton sectors, e.g. $G_l = K_4^{(S, T^3 ST^2 ST^3)}$ and $G_\nu = K_4^{(ST^2 ST^3 S, TST^4)}$, the lepton mixing matrix is determined to be of the row-column (RC) symmetric form [22, 23]

$$U_{RC} = \frac{1}{2} \begin{pmatrix} \phi & -1 & 1/\phi \\ -1 & -1/\phi & \phi \\ 1/\phi & \phi & 1 \end{pmatrix}. \quad (4.1)$$

The mixing angles are: $\sin^2 \theta_{12} = (3 - \phi)/5 \simeq 0.276$, $\sin^2 \theta_{23} = (2 + \phi)/5 \simeq 0.724$ and $\sin^2 \theta_{13} = (2 - \phi)/4 \simeq 0.0955$. Although this mixing pattern is not phenomenologically viable because of too large θ_{13} and θ_{23} , the first column of U_{RC} is still compatible with experimental data, and that is what we shall assume in the following.

The general principle of the Littlest seesaw is that different sectors of the Lagrangian preserve different residual subgroups of the flavor symmetry which is proposed in Ref. [15]. In this section, we shall consider the case that the electron, muon and tau sectors preserve different residual symmetries while the flavor symmetry is broken in the whole charged lepton Lagrangian, and the same holds true for the neutrino vacuum Φ_{atm} and Φ_{sol} . This scenario is schematically depicted in figure 6. Moreover we can generally write down the Littlest seesaw Lagrangian in the neutrino and charged lepton sectors as follows:

$$\begin{aligned} \mathcal{L} = & -y_{\text{atm}} \bar{L} \cdot \phi_{\text{atm}} N_R^{\text{atm}} - y_{\text{sol}} \bar{L} \cdot \phi_{\text{sol}} N_R^{\text{sol}} - \frac{1}{2} M_{\text{atm}} \overline{(N_R^{\text{atm}})^c} N_R^{\text{atm}} - \frac{1}{2} M_{\text{sol}} \overline{(N_R^{\text{sol}})^c} N_R^{\text{sol}} \\ & + y_\tau \bar{L} \cdot \varphi_\tau \tau_R + y_\mu \bar{L} \cdot \varphi_\mu \mu_R + y_e \bar{L} \cdot \varphi_e e_R + h.c., \end{aligned} \quad (4.2)$$

where φ_α ($\alpha = e, \mu, \tau$) can be Higgs fields transforming as triplets under the flavor symmetry

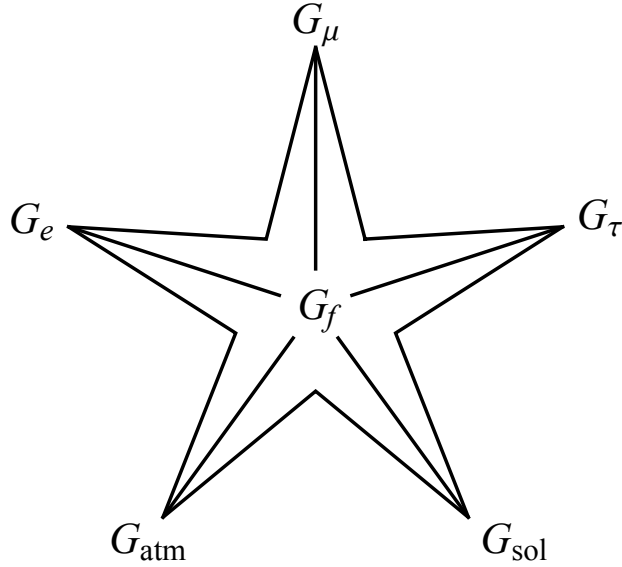


Figure 6: A sketch of the indirect model building approach, where the electron, muon and tau sectors preserve different residual subgroups G_e , G_μ and G_τ respectively, and the neutrino vacuum alignments Φ_{atm} and Φ_{sol} are enforced by the residual symmetries G_{atm} and G_{sol} respectively.

group, or the combination of the electroweak Higgs doublet with triplet scalar flavons. In order to obtain the above terms in a concrete model, the possible additional abelian symmetries are generically needed and they will not be specified here. It is generally more convenient to work in the charged lepton diagonal basis in practical model building. We show such an appropriate alternative basis in table 4. In this basis the charged lepton mass matrix is enforced to be diagonal by the chosen residual symmetries G_e , G_μ and G_τ in Eq. (4.5). The desired vacuum alignments in the charged lepton sector are

$$\langle \varphi_e \rangle = v_e \begin{pmatrix} 1 \\ 0 \\ 0 \end{pmatrix}, \quad \langle \varphi_\mu \rangle = v_\mu \begin{pmatrix} 0 \\ 1 \\ 0 \end{pmatrix}, \quad \langle \varphi_\tau \rangle = v_\tau \begin{pmatrix} 0 \\ 0 \\ 1 \end{pmatrix}. \quad (4.3)$$

If we regard φ_e , φ_μ , φ_τ as each being a triplet $\mathbf{3}$ of A_5 , then they each correspond to a different symmetry conserving direction of A_5 , with,

$$\rho_{\mathbf{3}}(S)\langle \varphi_e \rangle = \langle \varphi_e \rangle, \quad \rho_{\mathbf{3}}(T^3 ST^2 ST^3 S)\langle \varphi_\mu \rangle = \langle \varphi_\mu \rangle, \quad \rho_{\mathbf{3}}(T^3 ST^2 ST^3)\langle \varphi_\tau \rangle = \langle \varphi_\tau \rangle. \quad (4.4)$$

That is to say

$$G_e = Z_2^S, \quad G_\mu = Z_2^{T^3 ST^2 ST^3 S}, \quad G_\tau = Z_2^{T^3 ST^2 ST^3}. \quad (4.5)$$

Inserting these vacuum configurations in Eq. (4.3) into Eq. (4.2), we obtain the charged lepton mass matrix is diagonal with

$$m_\tau = y_\tau v_\tau, \quad m_\mu = y_\mu v_\mu, \quad m_e = y_e v_e. \quad (4.6)$$

The hierarchies among the three charged lepton masses are expected to be explained by including an extra $U(1)$ symmetry such that the effective Yukawa couplings y_τ , y_μ and y_e are of different order of magnitudes.

	S	T
1	1	1
3	$\begin{pmatrix} 1 & 0 & 0 \\ 0 & -1 & 0 \\ 0 & 0 & -1 \end{pmatrix}$	$\frac{1}{2} \begin{pmatrix} \phi & 1 & \phi-1 \\ -1 & \phi-1 & \phi \\ \phi-1 & -\phi & 1 \end{pmatrix}$
3'	$\begin{pmatrix} 1 & 0 & 0 \\ 0 & -1 & 0 \\ 0 & 0 & -1 \end{pmatrix}$	$\frac{1}{2} \begin{pmatrix} 1-\phi & \phi & 1 \\ \phi & 1 & 1-\phi \\ -1 & \phi-1 & -\phi \end{pmatrix}$
4	$\begin{pmatrix} -1 & 0 & 0 & 0 \\ 0 & -1 & 0 & 0 \\ 0 & 0 & 1 & 0 \\ 0 & 0 & 0 & 1 \end{pmatrix}$	$\frac{1}{4} \begin{pmatrix} -1 & -1 & 3 & \sqrt{5} \\ 1 & -3 & 1 & -\sqrt{5} \\ -3 & 1 & 1 & -\sqrt{5} \\ \sqrt{5} & \sqrt{5} & \sqrt{5} & -1 \end{pmatrix}$
5	$\begin{pmatrix} 1 & 0 & 0 & 0 & 0 \\ 0 & 1 & 0 & 0 & 0 \\ 0 & 0 & -1 & 0 & 0 \\ 0 & 0 & 0 & -1 & 0 \\ 0 & 0 & 0 & 0 & 1 \end{pmatrix}$	$\frac{1}{8} \begin{pmatrix} 1-3\phi & 2\phi^2 & 2/\phi^2 & -2\sqrt{5} & \sqrt{3}/\phi \\ -2\phi^2 & -4 & 4 & 0 & -2\sqrt{3}/\phi \\ -2/\phi^2 & 4 & 0 & 4 & -2\sqrt{3}\phi \\ -2\sqrt{5} & 0 & -4 & 4 & 2\sqrt{3} \\ \sqrt{3}/\phi & 2\sqrt{3}/\phi & 2\sqrt{3}\phi & 2\sqrt{3} & 3\phi-1 \end{pmatrix}$

Table 4: Alternative representation matrices of the generators S and T for the five irreducible representations of A_5 . This basis is more suitable to discuss the Littlest seesaw model in which the first column of the mixing matrix is in common with U_{RC} .

As regards the neutrino sector, the three columns of the U_{RC} mixing pattern read

$$\Phi_1 = \begin{pmatrix} \phi \\ -1 \\ 1/\phi \end{pmatrix}, \quad \Phi_2 = \begin{pmatrix} -1 \\ -1/\phi \\ \phi \end{pmatrix}, \quad \Phi_3 = \begin{pmatrix} 1/\phi \\ \phi \\ 1 \end{pmatrix}. \quad (4.7)$$

As schematically illustrated in figure 1, the solar alignment vector Φ_{sol} is orthogonal to Φ_1 , consequently its most general form is

$$\Phi_{\text{sol}} = \begin{pmatrix} x \\ 1+x\phi \\ \phi \end{pmatrix}. \quad (4.8)$$

This vacuum alignment Φ_{sol} would be enforced by some residual subgroup of A_5 for certain value of x ,

$$\begin{aligned} G_{\text{sol}} &= Z_5^{T^2ST}, & \text{for } x &= 0, \\ G_{\text{sol}} &= Z_2^{ST^2ST^3S}, & \text{for } x &= -1, \\ G_{\text{sol}} &= Z_2^{T^4(ST^2)^2}, & \text{for } x &= 1, \\ G_{\text{sol}} &= Z_3^{(T^2S)^2T^2}, & \text{for } x &= -1/\phi, \\ G_{\text{sol}} &= Z_3^{ST^3ST}, & \text{for } x &= -\phi. \end{aligned} \quad (4.9)$$

Furthermore the atmospheric alignment vector Φ_{atm} is along the direction of Φ_2 or Φ_3 which respects the following residual symmetry

$$G_{\text{atm}} = \begin{cases} Z_2^{ST^2ST^3S}, & \Phi_{\text{atm}} \propto \Phi_2, \\ Z_2^{T^4(ST^2)^2}, & \Phi_{\text{atm}} \propto \Phi_3. \end{cases} \quad (4.10)$$

In the following we consider the case of $\Phi_{\text{atm}} \propto \Phi_3$ ¹, then the Dirac neutrino mass matrix M_D and the right-handed neutrino mass matrix M_N are

$$M_D = \begin{pmatrix} a/\phi & xb \\ \phi a & (1 + \phi x)b \\ a & \phi b \end{pmatrix}, \quad M_N = \begin{pmatrix} M_{\text{atm}} & 0 \\ 0 & M_{\text{sol}} \end{pmatrix}. \quad (4.11)$$

Applying the seesaw formula results in the effective light neutrino mass matrix

$$m_\nu = m_a \begin{pmatrix} 2 - \phi & 1 & \phi - 1 \\ 1 & \phi + 1 & \phi \\ \phi - 1 & \phi & 1 \end{pmatrix} + m_b e^{i\eta} \begin{pmatrix} x^2 & x(x\phi + 1) & x\phi \\ x(x\phi + 1) & (x\phi + 1)^2 & \phi(x\phi + 1) \\ x\phi & \phi(x\phi + 1) & \phi + 1 \end{pmatrix}. \quad (4.12)$$

This neutrino mass matrix m_ν can be simplified into a quite simple form by performing a unitary transformation U_{RC} ,

$$m'_\nu = U_{RC}^T m_\nu U_{RC} = \begin{pmatrix} 0 & 0 & 0 \\ 0 & y & z \\ 0 & z & w \end{pmatrix} \quad (4.13)$$

with

$$\begin{aligned} y &= m_b e^{i\eta} (x - 1)^2, \\ z &= -m_b e^{i\eta} \phi (x^2 - 1), \\ w &= |w| e^{i\phi w} = 4m_a + m_b e^{i\eta} \phi^2 (x + 1)^2. \end{aligned} \quad (4.14)$$

The block diagonal neutrino mass matrix m'_ν of Eq. (4.13) can be easily diagonalized through the standard procedure, as shown in the appendix B. The lepton mixing matrix is predicted to take the form

$$U = \frac{1}{2} \begin{pmatrix} \phi & (1 - \phi) \sin \theta - e^{i\psi} \cos \theta & (\phi - 1) \cos \theta - e^{i\psi} \sin \theta \\ -1 & -\phi \sin \theta + e^{i\psi} (1 - \phi) \cos \theta & \phi \cos \theta + e^{i\psi} (1 - \phi) \sin \theta \\ \phi - 1 & -\sin \theta + e^{i\psi} \phi \cos \theta & \cos \theta + e^{i\psi} \phi \sin \theta \end{pmatrix} P_\nu, \quad (4.15)$$

with

$$P_\nu = \text{diag}(1, e^{i(-\psi+\rho)/2}, e^{i(-\psi+\sigma)/2}). \quad (4.16)$$

If we assign the left-handed lepton fields $L = (L_e, L_\tau, L_\mu)^T$ instead of $L = (L_e, L_\mu, L_\tau)^T$ to a triplet of the A_5 flavor group, and interchange the vacuum configurations $\langle \varphi_\mu \rangle$ and $\langle \varphi_\tau \rangle$ in Eq. (4.3), the resulting charged lepton mass matrix would be diagonal as well and the lepton mixing matrix can be obtained by exchanging the second and third rows of the PMNS

¹The experimental data on mixing angles and neutrino masses can not be accommodated for $\Phi_{\text{atm}} \propto \Phi_2$.

mixing matrix in Eq. (4.15). Furthermore, the exact results for the light neutrino masses are given by

$$\begin{aligned}
m_1^2 &= 0, \\
m_2^2 &= \frac{1}{2} \left[|y|^2 + |w|^2 + 2|z|^2 - \frac{|w|^2 - |y|^2}{\cos 2\theta} \right], \\
m_3^2 &= \frac{1}{2} \left[|y|^2 + |w|^2 + 2|z|^2 + \frac{|w|^2 - |y|^2}{\cos 2\theta} \right].
\end{aligned} \tag{4.17}$$

The expressions for the sine and cosine of rotation angle θ and the phases ψ , ρ , σ are

$$\begin{aligned}
\sin 2\theta &= \frac{2z e^{-i\eta} \sqrt{|y|^2 + |w|^2 + 2|y||w| \cos(\phi_w - \eta)}}{\sqrt{(|w|^2 - |y|^2)^2 + 4|z|^2 [|y|^2 + |w|^2 + 2|y||w| \cos(\phi_w - \eta)]}}, \\
\cos 2\theta &= \frac{|w|^2 - |y|^2}{\sqrt{(|w|^2 - |y|^2)^2 + 4|z|^2 [|y|^2 + |w|^2 + 2|y||w| \cos(\phi_w - \eta)]}}, \\
\sin \psi &= \frac{|w| \sin(\phi_w - \eta)}{\sqrt{|y|^2 + |w|^2 + 2|y||w| \cos(\phi_w - \eta)}}, \\
\cos \psi &= \frac{|y| + |w| \cos(\phi_w - \eta)}{\sqrt{|y|^2 + |w|^2 + 2|y||w| \cos(\phi_w - \eta)}}, \\
\sin \rho &= -\frac{(m_2^2 - |z|^2) \sin \eta + |y||w| \sin \phi_w}{m_2 \sqrt{|y|^2 + |w|^2 + 2|y||w| \cos(\phi_w - \eta)}}, \\
\cos \rho &= \frac{(m_2^2 - |z|^2) \cos \eta + |y||w| \cos \phi_w}{m_2 \sqrt{|y|^2 + |w|^2 + 2|y||w| \cos(\phi_w - \eta)}}, \\
\sin \sigma &= -\frac{(m_3^2 - |z|^2) \sin \eta + |y||w| \sin \phi_w}{m_3 \sqrt{|y|^2 + |w|^2 + 2|y||w| \cos(\phi_w - \eta)}}, \\
\cos \sigma &= \frac{(m_3^2 - |z|^2) \cos \eta + |y||w| \cos \phi_w}{m_3 \sqrt{|y|^2 + |w|^2 + 2|y||w| \cos(\phi_w - \eta)}}.
\end{aligned} \tag{4.18}$$

We can straightforwardly extract the mixing angles from Eq. (4.15) and find

$$\begin{aligned}
\sin^2 \theta_{13} &= \frac{3 - \phi}{8} + \frac{1 - \phi}{8} \cos 2\theta + \frac{1 - \phi}{4} \sin 2\theta \cos \psi, \\
\sin^2 \theta_{12} &= \frac{3 - \phi + (\phi - 1) \cos 2\theta + 2(\phi - 1) \sin 2\theta \cos \psi}{5 + \phi + (\phi - 1) \cos 2\theta + 2(\phi - 1) \sin 2\theta \cos \psi}, \\
\sin^2 \theta_{23} &= \frac{3 + (2\phi - 1) \cos 2\theta - 2 \sin 2\theta \cos \psi}{5 + \phi + (\phi - 1) \cos 2\theta + 2(\phi - 1) \sin 2\theta \cos \psi},
\end{aligned} \tag{4.19}$$

which fulfill the sum rule

$$4 \cos^2 \theta_{12} \cos^2 \theta_{13} = \phi^2. \tag{4.20}$$

If inserting the experimental best fit value $\sin^2 \theta_{13} = 0.0214$ [1], we arrive at

$$\sin^2 \theta_{12} \simeq 0.331, \tag{4.21}$$

which is in accordance with the experimental data [1]. As regards the Dirac CP phase, we find that the Jarlskog invariant takes a rather simple form,

$$J_{CP} = \frac{1}{16} \sin 2\theta \sin \psi, \tag{4.22}$$

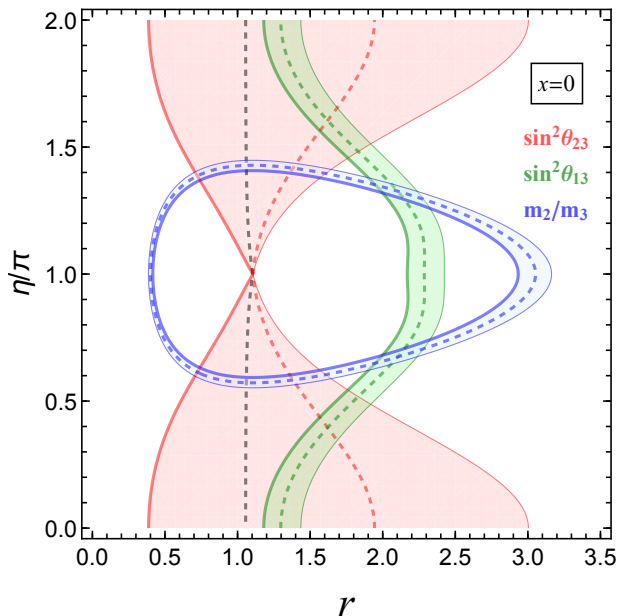


Figure 7: Contour plots of $\sin^2 \theta_{13}$, $\sin^2 \theta_{23}$ and m_2/m_3 in the $\eta - r$ plane for the Littlest seesaw model studied in section 4. Here we take $x = 0$ for which the solar vacuum alignment Φ_{sol} preserves the residual symmetry $G_{\text{sol}} = Z_5^{T^2 ST}$. The 3σ upper (lower) bounds of the lepton mixing angles are labelled with thick (thin) solid curves, and the dashed contour lines represent the corresponding best fit values. The 3σ ranges as well as the best fit values of the mixing angles are adapted from [1]. The black contour line refers to maximal atmospheric mixing angle with $\sin^2 \theta_{23} = 0.5$.

and an exact relation for $\cos \delta_{CP}$ in terms of the lepton mixing angles is satisfied,

$$\cos \delta_{CP} = \frac{(\phi - 1) \cos^2 \theta_{13} + [(5 + \phi) \sin^2 \theta_{13} - 3 + \phi] \cos 2\theta_{23}}{2\phi \sqrt{3 - \phi - 4 \sin^2 \theta_{13}} \sin 2\theta_{23} \sin \theta_{13}}. \quad (4.23)$$

For the Majorana invariant I_1 , we get

$$I_1 = \frac{2 - \phi}{64} \left\{ 4 \cos(\rho - \sigma) [\cos 2\theta \sin 2\psi - \sin 2\theta \sin \psi] + \sin(\rho - \sigma) [(\cos 4\theta + 3) \cos 2\psi - 2 \sin 4\theta \cos \psi - \sin^2 2\theta] \right\}. \quad (4.24)$$

If x is treated as a free parameter, the experimental data on lepton mixing can be described very well for certain values of x , η and $r = m_b/m_a$. On the other hand, if we require the solar vacuum alignment is associated with certain residual symmetry, as shown in Eq. (4.9), only $x = 0$ is phenomenologically viable. We show how the observables $\sin^2 \theta_{13}$, $\sin^2 \theta_{23}$ and m_2/m_3 vary in the $r - \eta$ plane in figure 7. In order to show concrete examples, we list the predictions for mixing parameters for some benchmark values of r and η in table 5 and table 6. Note that the atmospheric angle θ_{23} is outside of 3σ interval but quite close to 3σ bounds. We expect this discrepancy could be resolved by considering the contribution of the third almost decoupled right-handed neutrino of mass M_{dec} . Moreover, corrections to the leading order results are generally presented in an explicit model, and therefore it is not difficult to achieve good agreement with experimental data.

η	r	x	$\sin^2 \theta_{13}$	$\sin^2 \theta_{12}$	$\sin^2 \theta_{23}$	δ_{CP}/π	β/π	m_2^2/m_3^2
$\pm \frac{2\pi}{3}$	2.053	0	0.0223	0.331	0.304	∓ 0.424	± 0.282	0.0289
$\pm \frac{3\pi}{5}$	1.826	0	0.0249	0.329	0.355	∓ 0.351	± 0.200	0.0245
$\pm \frac{5\pi}{8}$	1.904	0	0.0241	0.329	0.337	∓ 0.376	± 0.228	0.0263
$\pm \frac{7\pi}{11}$	1.942	0	0.0236	0.330	0.328	∓ 0.388	± 0.242	0.0271
$\pm \frac{9\pi}{14}$	1.965	0	0.0234	0.330	0.323	∓ 0.396	± 0.250	0.0275
$\pm \frac{11\pi}{17}$	1.980	0	0.0232	0.330	0.320	∓ 0.400	± 0.256	0.0278
$\pm \frac{12\pi}{19}$	1.926	0	0.0238	0.330	0.332	∓ 0.383	± 0.236	0.0268
$\pm \frac{13\pi}{20}$	1.991	0	0.0231	0.330	0.317	∓ 0.404	± 0.259	0.0280
$\pm \frac{15\pi}{23}$	1.999	0	0.0230	0.330	0.316	∓ 0.406	± 0.262	0.0281
$\pm \frac{16\pi}{25}$	1.955	0	0.0235	0.330	0.325	∓ 0.392	± 0.246	0.0273
$\pm \frac{17\pi}{26}$	2.005	0	0.0229	0.330	0.314	∓ 0.408	± 0.265	0.0282
$\pm \frac{17\pi}{27}$	1.920	0	0.0239	0.329	0.333	∓ 0.381	± 0.234	0.0266
$\pm \frac{19\pi}{29}$	2.010	0	0.0228	0.330	0.313	∓ 0.41	± 0.266	0.0283
$\pm \frac{19\pi}{30}$	1.932	0	0.0238	0.330	0.330	∓ 0.385	0.238	0.0269

Table 5: Benchmark numerical results for the alternative Littlest seesaw model discussed in section 4.

η	r	x	$\sin^2 \theta_{13}$	$\sin^2 \theta_{12}$	$\sin^2 \theta_{23}$	δ_{CP}/π	β/π	m_2^2/m_3^2
$\pm \frac{2\pi}{3}$	2.050	0	0.0224	0.331	0.696	± 0.577	± 0.282	0.029
$\pm \frac{3\pi}{5}$	1.816	0	0.0251	0.329	0.644	± 0.65	± 0.199	0.0246
$\pm \frac{5\pi}{8}$	1.897	0	0.0243	0.329	0.662	± 0.625	± 0.227	0.0264
$\pm \frac{7\pi}{11}$	1.936	0	0.0238	0.33	0.671	± 0.612	± 0.241	0.0272
$\pm \frac{9\pi}{14}$	1.959	0	0.0235	0.33	0.676	± 0.605	± 0.249	0.0276
$\pm \frac{11\pi}{17}$	1.975	0	0.0233	0.33	0.68	± 0.6	± 0.255	0.0279
$\pm \frac{12\pi}{19}$	1.919	0	0.0240	0.329	0.668	± 0.618	± 0.235	0.0269
$\pm \frac{13\pi}{20}$	1.986	0	0.0232	0.33	0.682	± 0.597	± 0.259	0.0281
$\pm \frac{15\pi}{23}$	1.994	0	0.0231	0.33	0.684	± 0.594	± 0.262	0.0282
$\pm \frac{16\pi}{25}$	1.949	0	0.0236	0.33	0.674	± 0.608	± 0.245	0.0275
$\pm \frac{17\pi}{26}$	2.000	0	0.0230	0.33	0.685	± 0.592	± 0.264	0.0283
$\pm \frac{17\pi}{27}$	1.912	0	0.0241	0.329	0.666	± 0.62	± 0.232	0.0268
$\pm \frac{19\pi}{29}$	2.005	0	0.0229	0.33	0.686	± 0.591	± 0.266	0.0284
$\pm \frac{19\pi}{30}$	1.925	0	0.0239	0.329	0.669	± 0.616	± 0.237	0.027

Table 6: Benchmark numerical results for the alternative Littlest seesaw model discussed in section 4, where the second and third rows of the mixing matrix in Eq. (4.15) are exchanged.

5 Conclusion

The Littlest Seesaw approach assumes that a *different* residual flavour symmetry is preserved by each flavon, in the diagonal mass basis of two right-handed neutrinos, leading to a highly predictive set of possible flavon alignments for the charged leptons and neutrinos. The Littlest seesaw model can thereby give a successful description of both neutrino mixing and the light neutrino masses in terms of four input parameters. The case of S_4 , discussed in earlier work, leads to the lepton mixing matrix being predicted to be of the TM1 form. The neutrino mass spectrum is normal ordered and the lightest neutrino is massless. Moreover, CP violation in neutrino oscillation and leptogenesis arises from a unique single phase such that they are closely related. Therefore the Littlest seesaw model is quite predictive and attractive.

In this work, we have investigated whether the Littlest seesaw is confined to TM1 mixing, or is of more general applicability. We have performed a comprehensive analysis of possible lepton mixing which can be derived from the A_5 flavor symmetry group within the paradigm of the Littlest seesaw. The general principle of the Littlest seesaw is that different sectors of the Lagrangian preserve different residual subgroups of the flavor symmetry [15]. This idea is illustrated in figure 2 and figure 6. If the residual symmetry of the charged lepton sector is $G_l = Z_5^T$ which enforces the diagonality of the charged lepton mass matrix in the T generator diagonal basis, the subgroup $G_{\text{atm}} = Z_2^{T^3ST^2ST^3S}$ or $G_{\text{atm}} = Z_2^{T^3ST^2ST^3}$ is preserved by the atmospheric flavon, and solar flavon ϕ_{sol} breaks the flavor group A_5 into $G_{\text{sol}} = Z_3^{T^3ST^2S}$ or $G_{\text{sol}} = Z_3^{ST^2ST^3}$, the first column of the golden ratio mixing matrix is preserved. The experimental data on the lepton mixing angles and neutrino masses can be accommodated for certain values of the input parameters m_a , m_b and η except that the reactor angle θ_{13} is predicted to rather close to its 3σ boundary. This could be easily reconciled with the experimental results in an explicit model with small subleading corrections or by considering the third almost decoupled right-handed neutrino. Moreover, many numerical benchmark examples are found. The most remarkable point is $\eta = 0$ for $G_{\text{atm}} = Z_2^{T^3ST^2ST^3S}$ and $\eta = \pi$ for $G_{\text{atm}} = Z_2^{T^3ST^2ST^3}$, then both Dirac CP phase δ_{CP} and the atmospheric mixing angle θ_{23} would be exactly maximal. This mixing pattern is previously predicted in the semidirect approach of combining A_5 flavor symmetry with generalized CP [22, 27, 28], but here we have additional prediction for the neutrino masses and the generalized CP symmetry is not introduced at all.

In the same fashion we find a third golden Littlest seesaw model which preserves the first column of the U_{RC} mixing matrix in Eq. (4.1). Accordingly the residual subgroups in different sectors are $G_e = Z_2^S$, $G_\mu = Z_2^{T^3ST^2ST^3S}$, $G_\tau = Z_2^{T^3ST^2ST^3}$, $G_{\text{atm}} = Z_2^{T^4(ST^2)^2}$ and $G_{\text{sol}} = Z_5^{T^2ST}$. This case fits the experimental data well to a certain extent. The atmospheric angle θ_{23} is determined to lie outside the 3σ region although rather close to 3σ bounds. Generally corrections to the leading order results are expected to exist in an explicit model such that it is not difficult to achieve agreement with the data. Hence this golden Littlest seesaw model can be regarded as a good leading order approximation from the view of model building.

In conclusion, the Littlest seesaw is a general and predictive framework of explaining neutrino masses and lepton mixing. All the results of this paper only depend on the assumed residual symmetries and they are independent of the underlying mechanism which dynamically realizes the required vacuum alignments. It would be interesting to construct at least one of the above three golden Littlest seesaw models. Since all CP violation phases are

completely fixed in the golden Littlest seesaw model, another interesting question is whether the observed baryon asymmetry of the universe can be generated through leptogenesis and the resulting constraints on the right-handed neutrino masses.

Acknowledgements

G.-J. D. and C.-C. L. acknowledges the support of the National Natural Science Foundation of China under Grant No 11522546. S.F.K. acknowledges the STFC Consolidated Grant ST/L000296/1 and the European Union's Horizon 2020 research and innovation programme under the Marie Skłodowska-Curie grant agreements Elusives ITN No. 674896 and InvisiblesPlus RISE No. 690575. One of the author (G.-J. D.) is grateful to Chang-Yuan Yao for his kind help on plotting the figures.

Appendix

A Group Theory of A_5

A_5 is the group of even permutations of five objects, and it has $5!/2 = 60$ elements. Geometrically it is the symmetry group of a regular icosahedron. A_5 group can be generated by two generators S and T which satisfy the multiplication rules [21]:

$$S^2 = T^5 = (ST)^3 = 1. \quad (\text{A.1})$$

The 60 element of A_5 group are divided into 5 conjugacy classes:

$$\begin{aligned}
1C_1 &: 1 \\
15C_2 &: ST^2ST^3S, TST^4, T^4(ST^2)^2, T^2ST^3, (T^2S)^2T^3S, ST^2ST, S, T^3ST^2ST^3, \\
&\quad T^3ST^2ST^3S, T^3ST^2, T^4ST^2ST^3S, TST^2S, ST^3ST^2S, T^4ST, (T^2S)^2T^4 \\
20C_3 &: ST, TS, ST^4, T^4S, TST^3, T^2ST^2, T^2ST^4, T^3ST, T^3ST^3, T^4ST^2, TST^3S, T^2ST^3S, \\
&\quad T^3ST^2S, ST^2ST^3, ST^3ST, ST^3ST^2, (T^2S)^2T^2, T^2(T^2S)^2, (ST^2)^2S, (ST^2)^2T^2 \\
12C_5 &: T, T^4, ST^2, T^2S, ST^3, T^3S, STS, TST, TST^2, T^2ST, T^3ST^4, T^4ST^3 \\
12C'_5 &: T^2, T^3, ST^2S, ST^3S, (ST^2)^2, (T^2S)^2, (ST^3)^2, (T^3S)^2, (T^2S)^2T^3, \\
&\quad T^3(ST^2)^2, T^3ST^2ST^4, T^4ST^2ST^3, \quad (\text{A.2})
\end{aligned}$$

where nC_k denotes a class with n elements which have order k . The group structure of A_5 has been exhaustively analyzed in Ref. [21]. Following the convention of Ref. [21], we find that A_5 group has thirty-six abelian subgroups in total: fifteen Z_2 subgroups, ten Z_3 subgroups, five K_4 subgroups and six Z_5 subgroups. In terms of the generators S and T , the concrete forms of these abelian subgroups are as follows:

- Z_2 subgroups

$$\begin{aligned}
Z_2^{ST^2ST^3S} &= \{1, ST^2ST^3S\}, \quad Z_2^{TST^4} = \{1, TST^4\}, \quad Z_2^{T^4(ST^2)^2} = \{1, T^4(ST^2)^2\}, \\
Z_2^{T^2ST^3} &= \{1, T^2ST^3\}, \quad Z_2^{(T^2S)^2T^3S} = \{1, (T^2S)^2T^3S\}, \quad Z_2^{ST^2ST} = \{1, ST^2ST\}, \\
Z_2^S &= \{1, S\}, \quad Z_2^{T^3ST^2ST^3} = \{1, T^3ST^2ST^3\}, \quad Z_2^{T^3ST^2ST^3S} = \{1, T^3ST^2ST^3S\}, \\
Z_2^{T^3ST^2} &= \{1, T^3ST^2\}, \quad Z_2^{T^4ST^2ST^3S} = \{1, T^4ST^2ST^3S\}, \quad Z_2^{TST^2S} = \{1, TST^2S\}, \\
Z_2^{ST^3ST^2S} &= \{1, ST^3ST^2S\}, \quad Z_2^{T^4ST} = \{1, T^4ST\}, \quad Z_2^{(T^2S)^2T^4} = \{1, (T^2S)^2T^4\}.
\end{aligned}$$

All the above fifteen Z_2 subgroups are conjugate to each other.

- Z_3 subgroups

$$\begin{aligned}
Z_3^{T^3ST^2S} &= \{1, T^3ST^2S, ST^3ST^2\}, \quad Z_3^{TST^3S} = \{1, TST^3S, (ST^2)^2T^2\}, \\
Z_3^{T^3ST} &= \{1, T^3ST, T^4ST^2\}, \quad Z_3^{ST} = \{1, ST, T^4S\}, \\
Z_3^{(T^2S)^2T^2} &= \{1, (T^2S)^2T^2, (ST^2)^2S\}, \quad Z_3^{TST^3} = \{1, TST^3, T^2ST^4\}, \\
Z_3^{T^2ST^2} &= \{1, T^2ST^2, T^3ST^3\}, \quad Z_3^{TS} = \{1, TS, ST^4\}, \\
Z_3^{ST^3ST} &= \{1, ST^3ST, T^2(T^2S)^2\}, \quad Z_3^{ST^2ST^3} = \{1, ST^2ST^3, T^2ST^3S\}.
\end{aligned}$$

The ten Z_3 subgroups are related with each other by group conjugation.

R	Conjugacy Classes				
	$1C_1$	$15C_2$	$20C_3$	$12C_5$	$12C'_5$
1	1	1	1	1	1
3	3	-1	0	ϕ	$1 - \phi$
3'	3	-1	0	$1 - \phi$	ϕ
4	4	0	1	-1	-1
5	5	1	-1	0	0

Table 7: The character table of the A_5 group, where $\phi = \frac{1+\sqrt{5}}{2}$.

- K_4 subgroups

$$\begin{aligned}
K_4^{(ST^2ST^3S, TST^4)} &\equiv Z_2^{ST^2ST^3S} \times Z_2^{TST^4} = \{1, ST^2ST^3S, TST^4, T^4(ST^2)^2\}, \\
K_4^{(T^2ST^3, ST^2ST)} &\equiv Z_2^{T^2ST^3} \times Z_2^{ST^2ST} = \{1, T^2ST^3, (T^2S)^2T^3S, ST^2ST\}, \\
K_4^{(S, T^3ST^2ST^3)} &\equiv Z_2^S \times Z_2^{T^3ST^2ST^3} = \{1, S, T^3ST^2ST^3, T^3ST^2ST^3S\}, \\
K_4^{(T^3ST^2, TST^2S)} &\equiv Z_2^{T^3ST^2} \times Z_2^{TST^2S} = \{1, T^3ST^2, T^4ST^2ST^3S, TST^2S\}, \\
K_4^{(ST^3ST^2S, T^4ST)} &\equiv Z_2^{ST^3ST^2S} \times Z_2^{T^4ST} = \{1, ST^3ST^2S, T^4ST, (T^2S)^2T^4\}.
\end{aligned}$$

All the five K_4 subgroups are conjugate as well.

- Z_5 subgroups

$$\begin{aligned}
Z_5^{STS} &= \{1, STS, ST^2S, ST^3S, TST\}, & Z_5^{ST^3} &= \{1, ST^3, T^2S, (ST^3)^2, (T^2S)^2\}, \\
Z_5^{T^2ST} &= \{1, T^2ST, T^4ST^3, T^3(ST^2)^2, T^4ST^2ST^3\}, & Z_5^T &= \{1, T, T^2, T^3, T^4\}, \\
Z_5^{TST^2} &= \{1, TST^2, T^3ST^4, (T^2S)^2T^3, T^3ST^2ST^4\}, & Z_5^{ST^2} &= \{1, ST^2, T^3S, (ST^2)^2, (T^3S)^2\}.
\end{aligned}$$

All the six Z_5 subgroups are related to each other under group conjugation.

Here the superscript of a subgroup denotes its generator (or generators). The A_5 group has five irreducible representations: one singlet representation **1**, two three-dimensional representations **3** and **3'**, one four-dimensional representation **4** and one five-dimensional representation **5**.

The character table of A_5 group is reported in Table 7. We can straightforwardly obtain the Kronecker products between various representations:

$$\begin{aligned}
\mathbf{1} \otimes \mathbf{R} &= \mathbf{R} \otimes \mathbf{1} = \mathbf{R}, & \mathbf{3} \otimes \mathbf{3} &= \mathbf{1} \oplus \mathbf{3} \oplus \mathbf{5}, & \mathbf{3}' \otimes \mathbf{3}' &= \mathbf{1} \oplus \mathbf{3}' \oplus \mathbf{5}, & \mathbf{3} \times \mathbf{3}' &= \mathbf{4} \oplus \mathbf{5}, \\
\mathbf{3} \otimes \mathbf{4} &= \mathbf{3}' \oplus \mathbf{4} \oplus \mathbf{5}, & \mathbf{3}' \otimes \mathbf{4} &= \mathbf{3} \oplus \mathbf{4} \oplus \mathbf{5}, & \mathbf{3} \otimes \mathbf{5} &= \mathbf{3} \oplus \mathbf{3}' \oplus \mathbf{4} \oplus \mathbf{5}, \\
\mathbf{3}' \otimes \mathbf{5} &= \mathbf{3} \oplus \mathbf{3}' \oplus \mathbf{4} \oplus \mathbf{5}, & \mathbf{4} \otimes \mathbf{4} &= \mathbf{1} \oplus \mathbf{3} \oplus \mathbf{3}' \oplus \mathbf{4} \oplus \mathbf{5}, & \mathbf{4} \otimes \mathbf{5} &= \mathbf{3} \oplus \mathbf{3}' \oplus \mathbf{4} \oplus \mathbf{5}_1 \oplus \mathbf{5}_2, \\
\mathbf{5} \otimes \mathbf{5} &= \mathbf{1} \oplus \mathbf{3} \oplus \mathbf{3}' \oplus \mathbf{4}_1 \oplus \mathbf{4}_2 \oplus \mathbf{5}_1 \oplus \mathbf{5}_2. & & & & & & \text{(A.3)}
\end{aligned}$$

where **R** represents any irreducible representation of A_5 , and $\mathbf{4}_1$, $\mathbf{4}_2$, $\mathbf{5}_1$ and $\mathbf{5}_2$ stand for the two **4** and two **5** representations that appear in the Kronecker products.

B Diagonalization of a 2×2 symmetric complex matrix

If neutrinos are Majorana particles, their mass matrix is symmetric and generally complex. In the following, we present the result for the diagonalisation of a general 2×2 symmetric complex matrix, which is of the form

$$\mathcal{M} = \begin{pmatrix} a_{11}e^{i\phi_{11}} & a_{12}e^{i\phi_{12}} \\ a_{12}e^{i\phi_{12}} & a_{22}e^{i\phi_{22}} \end{pmatrix}, \quad (\text{B.1})$$

where a_{ij} and ϕ_{ij} ($i, j = 1, 2$) are real. It can be diagonalised by a unitary matrix U via

$$U^T \mathcal{M} U = \text{diag}(\lambda_1, \lambda_2), \quad (\text{B.2})$$

where the unitary matrix U can be written as

$$U = \begin{pmatrix} \cos \theta e^{i(\phi+\varrho)/2} & \sin \theta e^{i(\phi+\sigma)/2} \\ -\sin \theta e^{i(-\phi+\varrho)/2} & \cos \theta e^{i(-\phi+\sigma)/2} \end{pmatrix}, \quad (\text{B.3})$$

with the rotation angle θ satisfying

$$\tan 2\theta = \frac{2a_{12}\sqrt{a_{11}^2 + a_{22}^2 + 2a_{11}a_{22}\cos(\phi_{11} + \phi_{22} - 2\phi_{12})}}{a_{22}^2 - a_{11}^2}. \quad (\text{B.4})$$

The eigenvalues λ_1 and λ_2 can always set to be positive with

$$\lambda_1^2 = \frac{1}{2} \left\{ a_{11}^2 + a_{22}^2 + 2a_{12}^2 - \mathcal{S} \sqrt{(a_{22}^2 - a_{11}^2)^2 + 4a_{12}^2 [a_{11}^2 + a_{22}^2 + 2a_{11}a_{22}\cos(\phi_{11} + \phi_{22} - 2\phi_{12})]} \right\},$$

$$\lambda_2^2 = \frac{1}{2} \left\{ a_{11}^2 + a_{22}^2 + 2a_{12}^2 + \mathcal{S} \sqrt{(a_{22}^2 - a_{11}^2)^2 + 4a_{12}^2 [a_{11}^2 + a_{22}^2 + 2a_{11}a_{22}\cos(\phi_{11} + \phi_{22} - 2\phi_{12})]} \right\},$$

where $\mathcal{S} = \text{sign}((a_{22}^2 - a_{11}^2) \cos 2\theta)$. In the case of $\lambda_2 > \lambda_1$, i.e. $\mathcal{S} = 1$, the values of $\sin 2\theta$ and $\cos 2\theta$ are given by

$$\sin 2\theta = \frac{2a_{12}\sqrt{a_{11}^2 + a_{22}^2 + 2a_{11}a_{22}\cos(\phi_{11} + \phi_{22} - 2\phi_{12})}}{\sqrt{(a_{22}^2 - a_{11}^2)^2 + 4a_{12}^2 [a_{11}^2 + a_{22}^2 + 2a_{11}a_{22}\cos(\phi_{11} + \phi_{22} - 2\phi_{12})]}},$$

$$\cos 2\theta = \frac{a_{22}^2 - a_{11}^2}{\sqrt{(a_{22}^2 - a_{11}^2)^2 + 4a_{12}^2 [a_{11}^2 + a_{22}^2 + 2a_{11}a_{22}\cos(\phi_{11} + \phi_{22} - 2\phi_{12})]}}. \quad (\text{B.5})$$

Finally the phases ϕ , ϱ and σ are given by

$$\sin \phi = \frac{-a_{11} \sin(\phi_{11} - \phi_{12}) + a_{22} \sin(\phi_{22} - \phi_{12})}{\sqrt{a_{11}^2 + a_{22}^2 + 2a_{11}a_{22}\cos(\phi_{11} + \phi_{22} - 2\phi_{12})}} = \frac{\text{Im}(\mathcal{M}_{11}^* \mathcal{M}_{12} + \mathcal{M}_{22} \mathcal{M}_{12}^*)}{|\mathcal{M}_{11}^* \mathcal{M}_{12} + \mathcal{M}_{22} \mathcal{M}_{12}^*|},$$

$$\cos \phi = \frac{a_{11} \cos(\phi_{11} - \phi_{12}) + a_{22} \cos(\phi_{22} - \phi_{12})}{\sqrt{a_{11}^2 + a_{22}^2 + 2a_{11}a_{22}\cos(\phi_{11} + \phi_{22} - 2\phi_{12})}} = \frac{\text{Re}(\mathcal{M}_{11}^* \mathcal{M}_{12} + \mathcal{M}_{22} \mathcal{M}_{12}^*)}{|\mathcal{M}_{11}^* \mathcal{M}_{12} + \mathcal{M}_{22} \mathcal{M}_{12}^*|},$$

$$\sin \varrho = -\frac{(\lambda_1^2 - a_{12}^2) \sin \phi_{12} + a_{11} a_{22} \sin(\phi_{11} + \phi_{22} - \phi_{12})}{\lambda_1 \sqrt{a_{11}^2 + a_{22}^2 + 2a_{11}a_{22}\cos(\phi_{11} + \phi_{22} - 2\phi_{12})}},$$

$$\cos \varrho = \frac{(\lambda_1^2 - a_{12}^2) \cos \phi_{12} + a_{11} a_{22} \cos(\phi_{11} + \phi_{22} - \phi_{12})}{\lambda_1 \sqrt{a_{11}^2 + a_{22}^2 + 2a_{11}a_{22}\cos(\phi_{11} + \phi_{22} - 2\phi_{12})}},$$

$$\sin \sigma = -\frac{(\lambda_2^2 - a_{12}^2) \sin \phi_{12} + a_{11} a_{22} \sin(\phi_{11} + \phi_{22} - \phi_{12})}{\lambda_2 \sqrt{a_{11}^2 + a_{22}^2 + 2a_{11}a_{22}\cos(\phi_{11} + \phi_{22} - 2\phi_{12})}},$$

$$\cos \sigma = \frac{(\lambda_2^2 - a_{12}^2) \cos \phi_{12} + a_{11} a_{22} \cos(\phi_{11} + \phi_{22} - \phi_{12})}{\lambda_2 \sqrt{a_{11}^2 + a_{22}^2 + 2a_{11}a_{22}\cos(\phi_{11} + \phi_{22} - 2\phi_{12})}}. \quad (\text{B.6})$$

References

- [1] F. Capozzi, E. Di Valentino, E. Lisi, A. Marrone, A. Melchiorri and A. Palazzo, arXiv:1703.04471 [hep-ph].
- [2] G. Altarelli and F. Feruglio, Rev. Mod. Phys. **82**, 2701 (2010) doi:10.1103/RevModPhys.82.2701 [arXiv:1002.0211 [hep-ph]].
- [3] H. Ishimori, T. Kobayashi, H. Ohki, Y. Shimizu, H. Okada and M. Tanimoto, Prog. Theor. Phys. Suppl. **183**, 1 (2010) doi:10.1143/PTPS.183.1 [arXiv:1003.3552 [hep-th]].
- [4] S. F. King and C. Luhn, Rept. Prog. Phys. **76**, 056201 (2013) doi:10.1088/0034-4885/76/5/056201 [arXiv:1301.1340 [hep-ph]].
- [5] S. F. King, A. Merle, S. Morisi, Y. Shimizu and M. Tanimoto, New J. Phys. **16**, 045018 (2014) doi:10.1088/1367-2630/16/4/045018 [arXiv:1402.4271 [hep-ph]].
- [6] S. F. King, J. Phys. G **42**, 123001 (2015) doi:10.1088/0954-3899/42/12/123001 [arXiv:1510.02091 [hep-ph]].
- [7] S. F. King, Prog. Part. Nucl. Phys. **94** (2017) 217 doi:10.1016/j.pnpnp.2017.01.003 [arXiv:1701.04413 [hep-ph]].
- [8] P. Minkowski, Phys. Lett. B **67** (1977) 421; M. Gell-Mann, P. Ramond and R. Slansky in Sanibel Talk, CALT-68-709, Feb 1979, and in *Supergravity*, North Holland, Amsterdam (1979); T. Yanagida in *Proc. of the Workshop on Unified Theory and Baryon Number of the Universe*, KEK, Japan (1979); S.L.Glashow, Cargese Lectures (1979); R. N. Mohapatra and G. Senjanovic, Phys. Rev. Lett. **44** (1980) 912; J. Schechter and J. W. F. Valle, Phys. Rev. D **22** (1980) 2227.
- [9] S. F. King, Phys. Lett. B **439** (1998) 350 [hep-ph/9806440]; S. F. King, Nucl. Phys. B **562** (1999) 57 [hep-ph/9904210].
- [10] S. F. King, Nucl. Phys. B **576** (2000) 85 [hep-ph/9912492].
- [11] S. F. King, JHEP **0209** (2002) 011 [hep-ph/0204360].
- [12] P. H. Frampton, S. L. Glashow and T. Yanagida, Phys. Lett. B **548** (2002) 119 [hep-ph/0208157].
- [13] K. Harigaya, M. Ibe and T. T. Yanagida, Phys. Rev. D **86** (2012) 013002 [arXiv:1205.2198].
- [14] S. F. King, JHEP **1307**, 137 (2013) doi:10.1007/JHEP07(2013)137 [arXiv:1304.6264 [hep-ph]].
- [15] S. F. King, JHEP **1602**, 085 (2016) doi:10.1007/JHEP02(2016)085 [arXiv:1512.07531 [hep-ph]].
- [16] S. F. King and C. Luhn, JHEP **1609**, 023 (2016) doi:10.1007/JHEP09(2016)023 [arXiv:1607.05276 [hep-ph]].

- [17] P. Ballett, S. F. King, S. Pascoli, N. W. Prouse and T. Wang, *JHEP* **1703** (2017) 110 doi:10.1007/JHEP03(2017)110 [arXiv:1612.01999 [hep-ph]].
- [18] F. Bjorkerth, F. J. de Anda, I. de Medeiros Varzielas and S. F. King, *JHEP* **1506** (2015) 141 [arXiv:1503.03306]; F. Bjorkerth, F. J. de Anda, I. d. M. Varzielas and S. F. King, arXiv:1512.00850; F. Bjorkerth, F. J. de Anda, I. de Medeiros Varzielas and S. F. King, *JHEP* **1510** (2015) 104 [arXiv:1505.05504]; F. Bjorkerth, F. J. de Anda, S. F. King and E. Perdomo, arXiv:1705.01555 [hep-ph].
- [19] A. Datta, F. S. Ling and P. Ramond, *Nucl. Phys. B* **671**, 383 (2003) [arXiv:hep-ph/0306002].
- [20] Y. Kajiyama, M. Raidal and A. Strumia, *Phys. Rev. D* **76**, 117301 (2007) [arXiv:0705.4559 [hep-ph]].
- [21] G. J. Ding, L. L. Everett and A. J. Stuart, *Nucl. Phys. B* **857**, 219 (2012) doi:10.1016/j.nuclphysb.2011.12.004 [arXiv:1110.1688 [hep-ph]].
- [22] C. C. Li and G. J. Ding, *JHEP* **1505**, 100 (2015) doi:10.1007/JHEP05(2015)100 [arXiv:1503.03711 [hep-ph]].
- [23] R. de Adelhart Toorop, F. Feruglio and C. Hagedorn, *Nucl. Phys. B* **858**, 437 (2012) doi:10.1016/j.nuclphysb.2012.01.017 [arXiv:1112.1340 [hep-ph]].
- [24] F. Feruglio and A. Paris, *JHEP* **1103**, 101 (2011) doi:10.1007/JHEP03(2011)101 [arXiv:1101.0393 [hep-ph]].
- [25] L. L. Everett and A. J. Stuart, *Phys. Rev. D* **79**, 085005 (2009) doi:10.1103/PhysRevD.79.085005 [arXiv:0812.1057 [hep-ph]].
- [26] I. K. Cooper, S. F. King and A. J. Stuart, *Nucl. Phys. B* **875**, 650 (2013) doi:10.1016/j.nuclphysb.2013.07.027 [arXiv:1212.1066 [hep-ph]].
- [27] A. Di Iura, C. Hagedorn and D. Meloni, *JHEP* **1508**, 037 (2015) doi:10.1007/JHEP08(2015)037 [arXiv:1503.04140 [hep-ph]].
- [28] P. Ballett, S. Pascoli and J. Turner, *Phys. Rev. D* **92**, no. 9, 093008 (2015) doi:10.1103/PhysRevD.92.093008 [arXiv:1503.07543 [hep-ph]].
- [29] M. C. Chen and S. F. King, *JHEP* **0906** (2009) 072 [arXiv:0903.0125 [hep-ph]]; S. Choubey, S. F. King and M. Mitra, *Phys. Rev. D* **82** (2010) 033002 doi:10.1103/PhysRevD.82.033002 [arXiv:1004.3756 [hep-ph]]; S. F. King, *JHEP* **1101** (2011) 115 doi:10.1007/JHEP01(2011)115 [arXiv:1011.6167 [hep-ph]].
- [30] G. J. Ding, S. F. King and A. J. Stuart, *JHEP* **1312**, 006 (2013) doi:10.1007/JHEP12(2013)006 [arXiv:1307.4212 [hep-ph]].
- [31] C. Jarlskog, *Phys. Rev. Lett.* **55**, 1039 (1985).

- [32] G. C. Branco, L. Lavoura and M. N. Rebelo, Phys. Lett. B **180**, 264 (1986); J. F. Nieves and P. B. Pal, Phys. Rev. D **36**, 315 (1987). doi:10.1103/PhysRevD.36.315; J. F. Nieves and P. B. Pal, Phys. Rev. D **64**, 076005 (2001) doi:10.1103/PhysRevD.64.076005 [hep-ph/0105305]; E. E. Jenkins and A. V. Manohar, Nucl. Phys. B **792**, 187 (2008) [arXiv:0706.4313 [hep-ph]]; G. C. Branco, R. G. Felipe and F. R. Joaquim, Rev. Mod. Phys. **84**, 515 (2012) [arXiv:1111.5332 [hep-ph]].
- [33] S. F. King, J. Zhang and S. Zhou, JHEP **1612**, 023 (2016) doi:10.1007/JHEP12(2016)023 [arXiv:1609.09402 [hep-ph]].